

Chapter 2

Hexanitrohexaazaisowurtzitane (HNIW, CL-20)

Abstract Hexanitrohexaazaisowurtzitane, a nitroamine compound, has emerged as an important insensitive energetic material. This caged compound offers several interesting properties. This chapter discusses the properties and more importantly the formulations using CL-20.

2.1 Introduction

Hexanitrohexaazaisowurtzitane (HNIW), commonly known as CL-20, is 2,4,6,8,10,12-hexanitro-2,4,6,8,10,12-hexaazatetracyclododecane. It is a high-energy explosive compound and a polyazapolycyclic caged polynitramine. Structurally, it appears like two RDX molecules fused together. CL-20 is one of the most powerful explosives known today. Tests indicate that the formulations containing CL-20 have excellent stability, belong to hazard class 1.3, and environmentally friendly. It was first synthesized by Nielsen [1] in 1987 at the Naval Air Warfare Center, China Lake, CA, U.S.A. The strained/caged structure and high oxygen balance gives CL-20 a high density and high explosive power. The six N–NO₂ groups in CL-20 give a better oxidizer to fuel ratio and makes its performance better than RDX and HMX in specific impulse, detonation velocity, enthalpy of formation, and other parameters. It exists in five polymorphic forms, α , β , γ , ϵ , and ζ , and the existence of a polymorphic phase depends on the temperature and pressure. The ζ -form is formed at higher pressures. A sixth δ form has also been reported. Of these six forms, ϵ -polymorph has higher symmetry, thus morphologically more stable at room temperature and has the highest density (2.04 g/cm³) than the other polymorphs. Of the six forms, only β , γ , and ϵ have been prepared in the pure form. CL-20 has many applications including in propulsion of strategic missiles, space launchers and for high-lethality warheads for smart and light weapons, such as Precision Guided Missiles, and Laser Guided Bombs. The cost of producing CL-20 is decreasing and is less than \$800 per kg as reported by the USA Navy Mantech Report of 2003 [2].

2.2 Synthesis

The synthesis process may be divided into two steps. The first step involves the construction of the hexanitrohexaazaisowurtzitane cage, which is hexabenzylhexaazaisowurtzitane (HBIW). The chemical formula of HBIW is 2,4,6,8,10,12-hexabenzyl-2,4,6,12-hexaazatetracyclo[5, 5, 0, 05.9, 03.11] dodecane. HBIW is formed by the condensation reaction of glyoxal with benzylamine. Nielsen et al. [3] and Crampton et al. [4] suggested several derivatives of benzylamine to form cage. However, benzylamine provided the best yield for HBIW, about 80%. A number of solvents including acetonitrile, methanol, ethanol, and isopropyl alcohol have been tried to carry out the condensation reaction in the presence of an acid catalyst. However, acetonitrile is found to be the best solvent. The reaction can proceed in the temperature range of 0–25 °C [3]. Both organic and inorganic acids can be used as catalysts.

The second step involves nitrolysis. However, direct conversion of HBIW to CL-20 by nitrolysis cannot be carried out. The nitration of the phenyl rings is more favorable compared to the nitration of HBIW. Therefore, debenzylation of HBIW by catalytic hydrogenation prior to nitration is the preferred method. As a result, the functional groups associated with nitrogen atoms are substituted by the nitro groups.

The synthesis of CL-20 was first carried out by Nielsen and is described in the US Patent 5693794 [1]. Later Nielsen and his co-workers used a direct condensation of benzylamine with glyoxal. Crampton et al. [4] reported the synthesis of HNIW using the same route, which was the reaction of aldehydes with amines producing cage compounds. Both Nielsen et al. and Crampton et al. tried to find an alternative to benzylamine, but noted that the yield of HBIW was much lower. Debenzylation of HBIW is carried out in the presence of a catalyst. A variety of catalysts and nitrating agents have been explored. Nielsen and his co-workers used excess acetic anhydride for hydrogenation of HBIW forming 4,10-dibenzyl-2,6,8,12-tetraacetyl-2,4,6,8,10,12-hexaazaisowurtzitane (TADBIW) derivative. Several researchers employed Pd or Pd supported on carbon based catalyst in a variety of solvents for synthesis of HBIW derivatives. These include: Pd and Pd in formic acid as a solvent [5] H₂ and Pd/C in ethylbenzene [6], H₂, Pd/C, and acetic anhydride in the presence of N,N-dimethylacetamide [7]. However, the cost of palladium is an issue and should be optimized to lower the overall cost of synthesis. Other catalytic materials along with solvents used for synthesis are discussed below. Ou et al. [8] have substituted ethanol for acetonitrile. This not only reduces the cost but also the process is less toxic. In later papers, Ou et al. [9, 10] have described the synthesis of CL-20 using benzylamine and glyoxal. Their method included the condensation with formic acid in acetonitrile to give CL-20. Methods of synthesis and properties of CL-20 a highly energetic polycyclic nitramine are surveyed (Figs. 2.1 and 2.2). Yet in another paper, Wang et al. [12] describe a one-pot synthesis of HNIW. The starting material in this case is tetraacetyldibenzylhexaaza-isowurtzitane (TADBIW).

Nielson et al. [13] and Latypov et al. [14] synthesized CL-20 via TADBIW conversion to tetraacetyldinitrosohexaazaisowurtzitane (TADNIW) using N_2O_4 or NOBF_4 as catalyst. The resulting TADNIW was nitrated using NO_2BF_4 . A yield of 90% was reported. However, reagents NOBF_4 and NO_2BF_4 are costly, which are also not environmental friendly. A mixture of nitric and sulfuric acids was used by Hamilton et al. [15] and Bellamy [16] to nitrate both TADAIW and TADFIW to CL-20. Zhao et al. used 95–99% nitric acid for TADAIW nitration. The optimized reaction parameters provided 85% yield of CL-20. Surapaneni et al. [17] also used 98% nitric acid in order to improve process economics for the synthesis of CL-20.

Qian et al. [18] developed a sono-chemical method for the synthesis of CL-20 starting with TADBIW. The described two synthesis schemes using ultrasound at 30–80 kHz frequency in their experiments and obtained yields varying from 40 to 90%. The experiments were carried out at 333.15 K, mostly at 60 kHz frequency, and 10:5:1 ratio of HNO_3 , N_2O_4 , and TADBIW in ionic liquids. Their two reaction schemes are shown in Figs. 2.3 and 2.4.

Qian et al. [19, 20] continued the use of N_2O_4 as a nitrating agent in their subsequent work and reported good yield of CL-20. Sung et al. [21] studied the reaction mechanism of nitration/nitrolysis of tetraacetylhexaazaisowurtzitane (TAIW) with the mixture of nitric acid and sulfuric acid. According to them, two free secondary amines of TAIW are nitrated first and then four acetyl groups of TAIW, which were dependent on temperature.

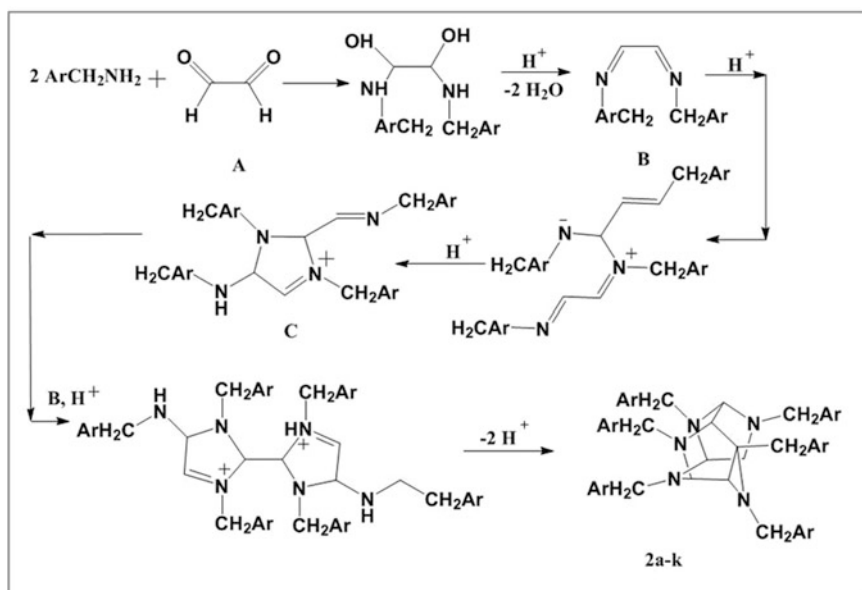


Fig. 2.1 Synthesis mechanism for this reaction is in scheme [11]. Ar = Ph (a), $\text{C}_6\text{H}_4\text{Me-p}$ (b), $\text{C}_6\text{H}_4\text{Me-o}$ (c), $\text{C}_6\text{H}_4\text{OMe-p}$ (d), $\text{C}_6\text{H}_4\text{OMe-o}$ (e), $\text{C}_6\text{H}_3(\text{OMe})_{2,3,4}$ (f), $\text{C}_6\text{H}_4\text{Pri-p}$ (g), $\text{C}_6\text{H}_4\text{Cl-p}$ (h), $\text{C}_6\text{H}_4\text{Cl-o}$ (i), $\text{C}_6\text{H}_4\text{F-o}$ (j), $\text{C}_6\text{H}_4\text{Br-o}$ (k)

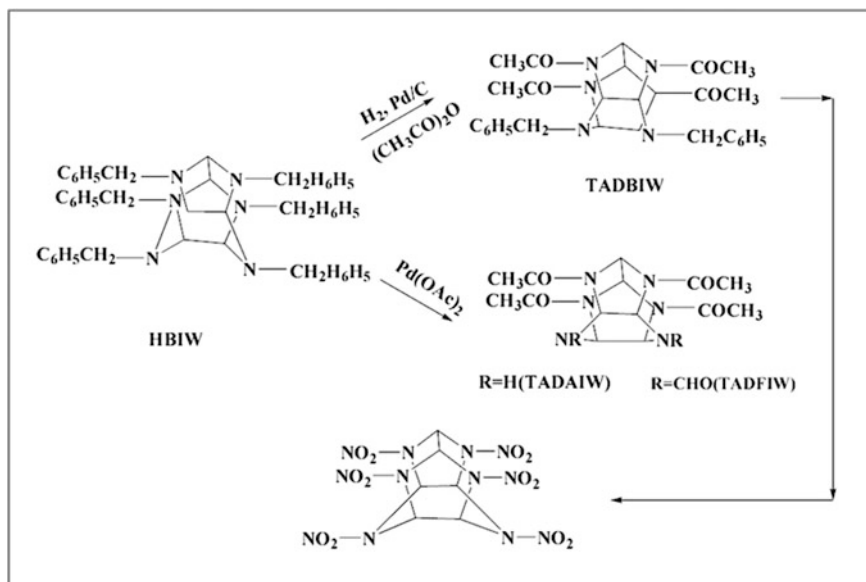


Fig. 2.2 Synthesis of hexanitrohexaazaisowurtzitane (CL-20) [3] and CL-20-based formulations

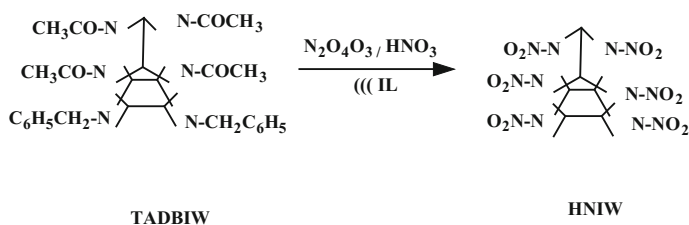


Fig. 2.3 Overall reaction scheme (Qian et al. [18, 20])

Gore et al. [22] described a method for synthesis of CL-20 from 2, 6, 8, 12-tetraacetyl-4, and 10-dibenzylhexaazaisowurtzitane using debenzylation followed by nitration. Reaction of TADBIW with cerium (IV) ammonium nitrate produced the debenzylated product, which on nitration with $\text{HNO}_3/\text{H}_2\text{SO}_4$ resulted in CL-20. Acetylation of the debenzylated and further nitration also resulted in CL-20. Kawabe et al. [23], and Cagnon et al. [24] patented their synthesis process for production of CL-20. Cagnon et al. synthesized hexanitrohexaaza-isowurtzitane, in a single reaction stage, by nitration of the substituted hexa-azaisowurtzitane derivative formed by reaction of the α , β -dicarbonyl derivative with the primary amine. They claimed that this route reduced the cost by eliminating the intermediate step of making HBIW and eliminating the expensive stage of catalytic hydrogenolysis. Kawabe et al. [23] used an expensive palladium catalyst.

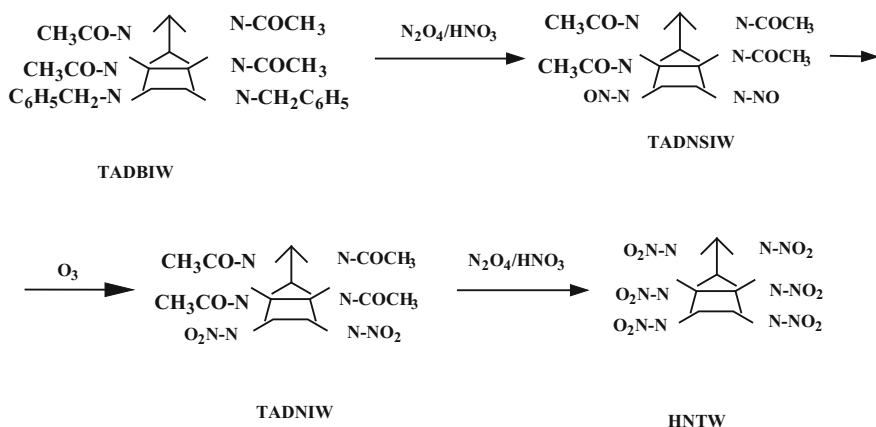


Fig. 2.4 Actual reaction scheme showing the intermediates [20]

In the one-pot synthesis process for HNIW described by Wang et al. [12] the starting material was TADBIW. A yield up to 82% and a purity of CL-20 up to 98% was claimed by the authors. This one pot method is based on the method described earlier by Latpov et al. [25]. This is a two stage process involving nitrosation followed by nitration in which 2,6,8,12-tetraacetyl-4,10-dibenzyl-2,4,6,8,10,12-hexaazaisowurtzitane is converted to 2,4,6,8,10,12-hexanitro-2,4,6,8,10,12-hexaazaisowurtzitane, and it is claimed that the product is better than 95% pure. Pang et al. [26] describe a synthesis route in which hexabenzylhexaazaisowurtzitane is converted to HNIW and avoided the hydrogenolysis step. Although the route of oxidative debenzylation and acetylation is less expensive, the yield is less than the conventional process.

Chapman and Hollins [27] described the oxidation of hexa(1-pro-pentyl)hexaazaisowurtzitane [HPIW] by singlet oxygen. This synthesis route is a modified procedure suggested by Herve et al. [28], although they did not synthesize CL-20. They presented a general method for the synthesis of hexaazaisowurtzitane cages avoiding the condensation of benzylamines. Some of the compounds synthesized by these authors could act as precursors for the preparation of CL-20. The procedure consists of the synthesis of hexaallylhexaazaisowurtzitane, followed by its conversion to HPIW, and finally to HNIW. The authors present different routes to the synthesis of HPIW and different photooxidation routes to convert HPIW to HNIW.

The effect of several process variables and their optimization has been discussed by Mandal et al. [29]. Their study noted that for approximate 85% yield, optimized temperature range was 345–358 K, nitric acid concentration range from 98 to 92%, reaction time of 1 h, and temperature during the addition of TAIW into the mixed acid to be in the range of 298–313 K. To improve the particle size of CL-20, during the recrystallization process, the authors have studied the effect of parameters like addition rate of anti-solvent and rate of agitation and identified optimum conditions.

Purification, recrystallization, and nano particle synthesis of CL-20 have received a greater attention in recent years. The importance of different polymorphs and particle size in the use of CL-20 as an insensitive explosive have been discussed by several authors [30–34].

In an unusual study of crystal transition, Song et al. [21] have looked at the effect of solvents on crystal transformation. ε -CL-20 was recrystallized from pure (alcohol, dichloro-methane, acetone and ethyl acetate) and mixed (alcohol-acetone, alcohol-ethylacetate, dichloromethane-acetone, dichloromethane-ethyl acetate and acetone-ethyl acetate with different volume ratio) solvents. The resulting crystal forms were characterized by Fourier Transform Infrared Spectroscopy (FTIR) and Scanning Electron Microscope (SEM).

Several authors have reviewed the synthesis of CL-20. They are: Ou et al. [8, 9], Sysolyatin [11], Agrawal [35], and Nair et al. [36]. Chapman et al. [37] investigated the synthesis of CL-20 as a part of their work for SERDP. Their procedure does not involve benzylamine glyoxal condensation, a procedure followed by many investigators. A synthesis method starting from tetracetyldi-formylhexaazaisowurtzitane (TADFIW) has been described by Jin et al. [38] in which γ -HNIW was first produced and then was converted to ε -CL-20 in the solution in which nitration reaction occurred. The yield of ε -CL-20 was 91%, and the purity close to 99.5%. Duddu and Dave [39] proposed a method to transform all other polymorphs to ε -HNIW using acetic acid and ethyl acetate as mixed solvent, and n-hexane as nonsolvent.

2.2.1 Characterization of Polymorphs of CL-20

The ε -HNIW has the highest density among all other polymorphs and thermodynamically most stable at ambient conditions. As a result, the focus is to synthesize ε -HNIW with a maximum yield. Various properties of CL-20 polymorphs are given in Table 2.1. As shown in Table 2.1, these polymorphs differ from each other in the spatial orientation of the nitro groups relative to the five- and six-membered rings of the cage, the type of the crystal packing and the number of molecules per unit cell [11].

Wardle and Hinshaw [40] discussed the formation of α -, β -HNIW, which mainly depended on the solution used for recrystallization or precipitation of HNIW. The α -HNIW was formed upon precipitation of HNIW with chloroform from its solutions in sulfolane. They noted the presence of β -HNIW when crude HNIW was recrystallized from benzene solution. However, β -HNIW is very unstable and converts readily to γ -HNIW at 185 °C. γ -HNIW can also be synthesized by the nitrolysis of the diformyl derivative with nitric acid. Direct synthesis of δ -HNIW is not known. Although Wardle and Hinshaw initially reported that the heating of γ -HNIW at 230 °C changes it to δ -HNIW. Later, based on IR spectroscopic data, they suggested it was a structural modification rather than the formation of δ -HNIW, which is stable only at elevated pressures, and was detected during the

Table 2.1 Property and CL-20 polymorphs [11]

Property	Polymorph			
	α	β	γ	ε
Orientation of the NO ₂ groups at the N(4) and N(10) Atoms	<i>exo, exo</i>	<i>exo, exo</i>	<i>exo, exo</i>	<i>exo, endo</i>
Number of molecules per unit cell	8	4	4	4
Space group	<i>Pbca</i>	<i>Pb2_{1a}</i>	<i>P2_{1/n}</i>	<i>P2_{1/n}</i>
Symmetry	Orthorhombic	Orthorhombic	Monoclinic	Monoclinic
Crystal habitus	Prisms	Needles	Plates	Prisms
Decomposition temperature, °C	260	260	260	260
Polymorphic transition temperature (and type), °C	–	185 ($\beta \rightarrow \gamma$)	230 ($\gamma \rightarrow \delta$)	–
Density (g cm ⁻³)	1.961 (2.001) ^a	1.985	1.916	2.04

^a The value is given for the hemihydrate of the α Polymorph

equilibrium transformation of the γ -phase. Russel et al. [41] reported the presence of ζ -HNIW at a high pressure during a reversible phase transition of the γ -polymorph at a pressure of (0.7 ± 0.05) GPa.

Ciezek et al. [42] examined the high pressure transition of ε to γ -CL-20 at room temperature and at pressures up to 27 GPa. They obtained the vibrational spectra of polycrystalline material and their recorded Raman spectra are shown in Fig. 2.5.

Raman profiles shown are vertically scaled for the sake of clarity. The main region covered is from 200 to 1100 cm⁻¹, and the range between 1200 and 1400 cm⁻¹ is omitted. The omission in this range is explained as dominance due to strong first-order scattering from the diamond anvils. The authors apparently omitted

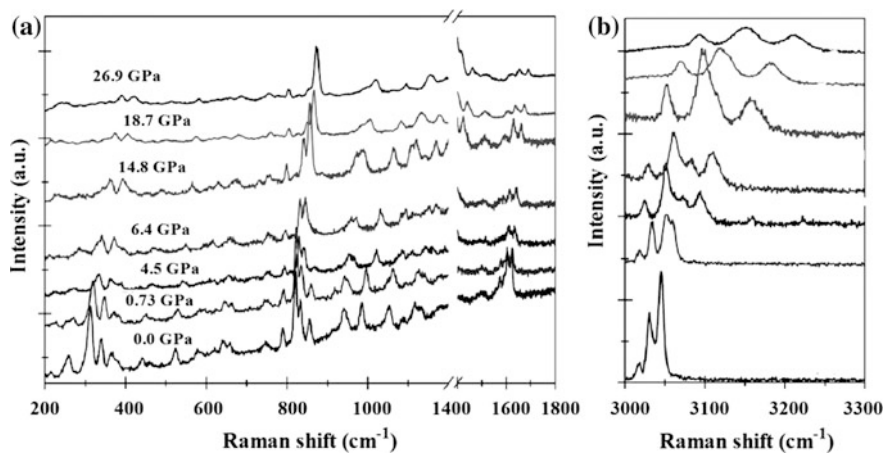


Fig. 2.5 Typical Raman spectra of CL-20 in the frequency range of 200–1800 cm⁻¹ (a) and 3000–3300 cm⁻¹ (b) [42]

the spectral region between 1800 and 3000 cm^{-1} as the vibrational intensity in this range was low. Based on their experimental data, they concluded that the $\varepsilon \rightarrow \gamma$ transition is purely conformational and that both the crystallographic space group and number of molecules per unit cell are retained. They also suggest the existence of $\gamma \rightarrow \delta$ transition at 18.7 GPa. It is clear that the spectra are pressure-induced, and the pressure effect is prominent in the 200–400 frequency range

Gump and Peiris [43] also investigated the phase transition as a function of pressure and temperature. They noted that ε -HNIW was stable under ambient pressure to a temperature of 120 °C. A phase transition to the γ -HNIW was observed at 125 °C and the γ -HNIW remained stable until thermal decomposition above 150 °C. The XRD measurements used to follow the phase transition are shown in Fig. 2.6. They fitted the pressure-volume data for the ε -HNIW phase at ambient and 75 °C by the Birch–Murnaghan formalism to obtain isothermal equations of state.

Turcotte et al. [44] explored the phase transitions using a DSC system. The DSC curve is shown in Fig. 2.7. They noticed the presence of two peaks. The peak at $T_p = 162 \pm 1$ °C was assigned to a solid–solid phase transition from $\varepsilon \rightarrow \gamma$. The peak at 141 ± 1 °C could not be assigned to any polymorph as there was no reference of such a peak in the literature. Ghosh et al. [45] using raw CL-20 prepared ε -CL-20 and provide density, X-ray diffraction patterns, FTIR and Raman frequencies, DSC curve as a part of the characterization of ε -CL-20.

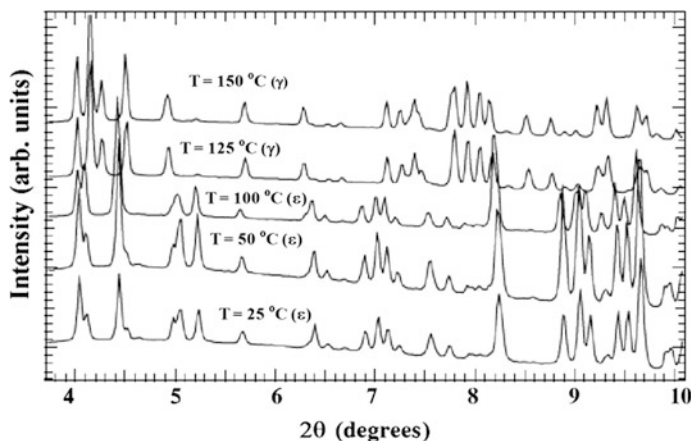


Fig. 2.6 Phase change from ε to γ upon heating at ambient pressure [43]

Fig. 2.7 Endothermic phase transition of CL-20: DSC, $5\text{ }^{\circ}\text{C min}^{-1}$, pinhole pan, in nitrogen: **a** 0.2 mg heated from 30 to $190\text{ }^{\circ}\text{C}$; **b** 5 mg with a 1 h isothermal step at $140\text{ }^{\circ}\text{C}$ [44]

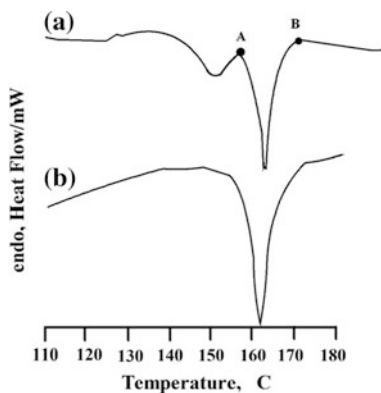
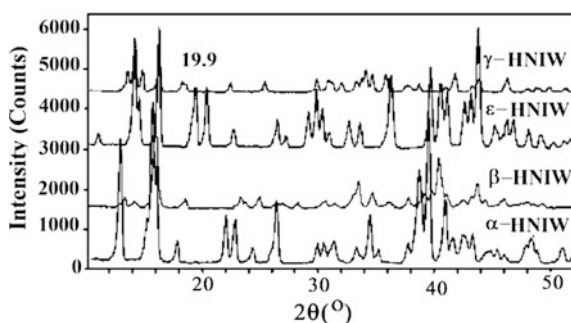


Fig. 2.8 XRD patterns of phase change of HNIW [47]



2.2.2 Diffraction Studies

The XRD pattern is a valuable information for identifying a compound and its polymorph. As discussed in the previous section (Fig. 2.8) the XRD was used to understand the transition of ϵ -HNIW to γ -HNIW. Meents et al. [46] investigated electron density of the ϵ -polymorph of CL-20 based on high-resolution X-ray single-crystal diffraction experiments at low temperature using synchrotron radiation. The crystals were made by recrystallization from a solution in which ϵ -HNIW was dissolved in propanol. Based on their experimental studies and model fitting, the authors discuss the chemical bonding and come to the conclusion that there is no evidence to support that electron-density maxima near the C-NO₂ bonds mapped on the electron-density isosurface can be correlated with impact sensitivities. The experimental results compared well with the DFT calculated bond-topological properties.

Chen et al. [47] studied in detail the XRD pattern of α -HNIW, β -HNIW, γ -HNIW, and ε -HNIW. The data are shown in Fig. 2.8 that covered 2θ from 10 to 50° . According to the authors, diffraction peaks for all four polymorph were not observed above 50° . There are more than 20 diffraction peaks in each XRD pattern of α -, β -, γ -, and ε -HNIW, respectively, some of which had overlapping peaks (Table 2.2).

Table 2.2 Important diffraction information of α -, β -, γ -, and ε -HNIW crystals [47]

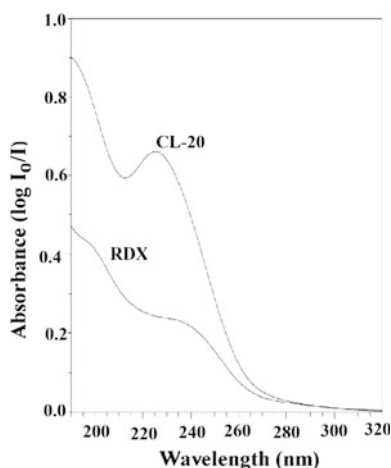
Analytic	Crystallographic parameters	2θ ($^\circ$)	D (hkl)	I%
ε -HNIW	Crystal system:	12.6	12.5	94.0
	Monoclinic	12.8	6.9	41.0
	Space group: P21/a	13.8	6.4	94
	a (nm) 1.3748	15.7	5.6	40
	b (nm) 1.2596	19.9	4.4	20
	c (nm) 0.8867	22.0	4.0	46
	α ($^\circ$) 90	25.8	3.5	52
	β ($^\circ$) 111.9	27.8	3.2	61
α -HNIW	γ ($^\circ$) 90	29.9	3.0	47
	Crystal system:			
	Orthorhombic			
	Space group: Pbca	12.1	7.3	77.0
	a (nm) 0.9478	13.8	6.4	100
	b (nm) 1.3206,	15.1	5.9	36.0
	c (nm) 2.356	20.2	4.4	40
	α ($^\circ$) 90	28.0	3.2	67.0
β -HNIW	Crystal system:			
	Orthorhombic			
	Space group: Pca21	13.6	6.5	89.0
	a (nm) 0.9652	13.7	6.5	100
	b (nm) 1.1644	24.2	3.7	21.0
	c (nm) 1.3002	28.3	3.2	28.0
γ -HNIW	Crystal system:	13.9	6.3	43.8
	Monoclinic	14.5	6.1	100
	Space group: P21/n	15.2	5.8	41.5
	a (nm) 1.3213	16.5	5.3	64.1
	b (nm) 0.8161	18.6	4.8	22.6
	c (nm) 1.4898	22.8	3.9	19.1
	α ($^\circ$) 90	34.4	2.6	37.9
	β ($^\circ$) 109.12	36.1	2.5	37.9
	γ ($^\circ$) 90	42.1	2.1	40.0

2.3 Detection

The main focus on the detection of CL-20 is from water and soil. One of the issues related to its detection is the fragmentation and decomposition of CL-20 in the liquid medium including water. Cabalo and Sausa [48], by using a surface laser photo-fragmentation- fragment detection (SPF-FD) spectroscopy at ambient temperature and pressure, were able to detect various explosives including CL-20 in the concentration range of 1–15 ng/cm² at 1 atm and room temperature. They used a low power, 248-nm laser photo-fragments the target molecule on the surface of a substrate, and a low power, 226-nm laser ionizes the resulting nitric oxide fragment by resonance-enhanced multi-photon ionization by means of its A-X (0,0) transitions near 226 nm. The lower limit of detection for CL-20 was 7.1 ng/cm² at 248 nm. A HPLC coupled with a UV detector is used frequently to identify and quantify CL-20 in a solution. As noted by Larson et al. [49] the detection of CL-20 in a variety of environmental samples requires matrix-specific sample preparation, separation by reverse-phase high performance liquid chromatography, and ultra-violet detector. Also, most of these methods follow USEPA SW-846 Method 8330 for the determination of explosives in waters and soils. Using a chromatographic column and UV-VIS detector, Larson et al. separated and detected CL-20 from the solution [49]. The UV spectrum of CL-20 in acetonitrile is shown in Fig. 2.9.

A number of researchers have used a combination of HPLC and various other detectors to detect CL-20 [50, 51]. Anthony et al. [52] used EPA 8330A method to detect CL-20 in soil samples. The HPLC was equipped with a Supelcosil LC-CN column for separation of CL-20 and a Diode Array Detector set at 230 nm (Imax) was used for detection of CL-20. An ultra HPLC also appears to be promising for separation of energetic materials including CL-20 [53]. Oehrle [54] used USEPA SW-846 Method 8330 for analysis of CL-20 in the presence of 14 nitroaromatics and nitramine. Along with HPLC, he used a photodiode array detection system for

Fig. 2.9 Absorbance curve of 2.25×10^{-3} M RDX and CL-20 in the 190- to 290-nm range [48]



CL-20 peak identification. The analysis for CL-20 was accomplished in less than 30 min using an isocratic HPLC mobile phase of water and isopropanol.

Persson et al. [55] used a HPLC method for qualitative and quantitative analysis of a mixture of RDX, 2,4,6-TNT, 2,4-DNT, HMX, PETN, Tetryl, HNS, TNAZ and HNIW. A programmable multi-wavelength detector in the UVNIS range was used for detection of these explosives in less than 10 min. The detection limit for HNIW was less than 5 ng.

NMR characterization has been carried out [56] and coupling constants have been determined. Agilent Technologies proposed a APCI LC/MS/MS based methods for detection of TNT, RDX, and CL-20. According to them, CL-20 yields two intense product ions. The major product ion is m/z 154 or a loss of 319 mass units ($C_5H_5O_8N_9$). The mass spectrum is given in Fig. 2.10.

2.4 Physical and Thermal Properties

Physical, and thermal properties of CL-20 are given in Table 2.3. In addition to the data presented in this table, other properties such as solubility, vapor pressure, ideal gas heat capacity and entropy are also discussed in the following sections (Tables 2.4 and 2.5)

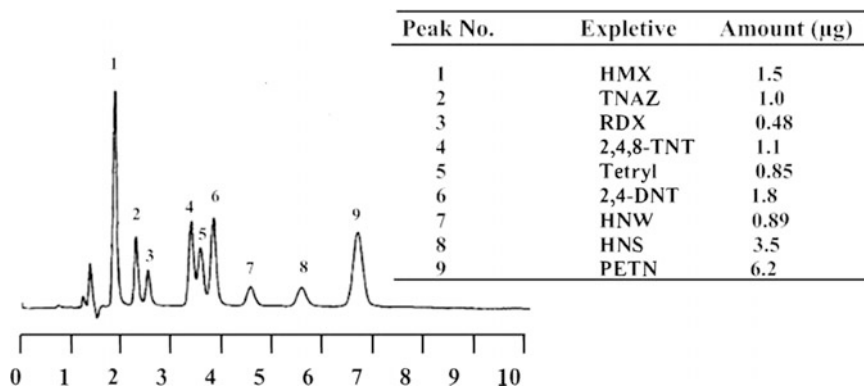


Fig. 2.10 HPLC chromatogram for a nine compound explosive mixture (measurement parameters as in Table) [55]

Table 2.3 Properties of CL-20

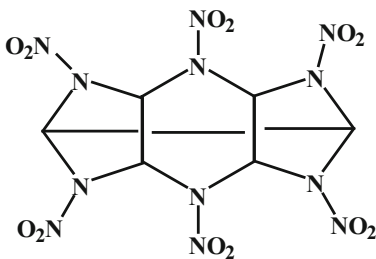
CAS number	135285-90-4
IUPAC name	5,2,6-(Iminomethenimino)-1H-imidazo[4,5-b]pyrazine, octahydro-1,3,4,7,8,10-hexanitro-
Other names	2,4,6,8,10,12-Hexanitro-2,4,6,8,10,12-hexaazatetracyclododecane; 2,4,6,8,10,12-Hexanitrohexaazaisowurtzitane; CL 20; HNIW; Hexanitrohexaazaisowurtzitane; LX 19; RX 39AB; RX 39AC
Chemical structure	
Molecular mass	438.23, Daltons
Density	2.04, g/cm ³ @ 298.15 K
Melting point	513 K [57]
Boiling point	862 K [57]
Acentric factor	2.347 [57]
Critical temperature	1058 K [57]
Critical pressure	48.9 bar [57]
Dipole moment	1.016 debye [58]
Enthalpy of fusion	13.7 [57] and 42.7 [59] kJ/mole
Enthalpy of formation (gas phase)	141.0 kcal/mole
Enthalpy of sublimation	150–170 kJ/mole
Enthalpy of vaporization	–311 kJ/mole
Aqueous solubility	3.86 ^{–3} ; 2.91 ^{–3} g/l @ 298.15 K [60]
Log K _{OW}	1.92 [51] 1.375 and 4.14 {Predicted values}

Table 2.4 Enthalpy of combustion and formation [61]

Material	$\Delta H_{\text{combustion}}$ (10 ⁶ J/mol)	$\Delta H_{\text{formation}}$ (10 ³ J/mol)
β-CL-20	–3.649	+431.0 ± 13
ε-CL-20	–3.596	+377.4 ± 13

Table 2.5 Enthalpy of detonation of CL-20 [61]

Material	$\rho(\text{g/cm}^3)$	$J/\text{g}^{(a)}$	J/cm^3	$\text{TMD}^{(b)} J/\text{J/cm}^3$
ε -CL-20	1.96 Expt.	6.234 ± 63	$12,219 \pm 123$	$12,717 \pm 129$
ε -CL-20	1.96 Calc.	6.029 ± 146	$11,817 \pm 286$	$12,301 \pm 298$

^(a) 25 °C, $\text{H}_2\text{O}^{(\text{liquid})}$ ^(b) TMD is the theoretical maximum density

2.4.1 Vapor Pressure

Only a few experimental vapor pressure data are reported in the literature. Greenlief et al. [62] obtained the data at the low pressure range using the Knudsen effusion method. The data are shown in Table 2.6.

Sinditskii et al. [63] while determining the kinetic parameters of combustion of four solid rocket propellant oxidizers and other energetic compounds also obtained the vapor pressure data including that of CL-20 above 600 K. Sinditskii et al. compiled the vapor pressure data for CL-20 from the literature (see Fig. 2.11), and noted significant differences in the reported values.

Both Greenlief et al. [62] and Sinditskii et al. [63] correlated the vapor pressure data according to a Clausius-Clapeyron type equations. The equations along with their best fit constants are given below:

$$\text{Solid: } \ln P = 25.328 - \frac{17,715}{T}, \text{ (for 660–775 K)}$$

$$\text{Liquid: } \ln P = 19.337 - \frac{13,085}{T}, \text{ (for 775–960 K)}$$

The equation provided by Greenlief is given below:

$$\ln P = 9.552 - \frac{9087.9}{T}$$

This equation provided a maximum deviation of 5% and an average absolute deviation of 4%.

Boddu et al. [64] calculated the vapor pressure of CL-20 using an equation of state approach. However, their predicted values are an order of magnitude lower compared to our experimental data [62].

Table 2.6 Experimental vapor pressure data, P in Pascals. [62]

Temperature (K)	383.15	393.15	395.15	405.15	405.15
Vapor pressure (Pa)	7.067^{-07}	1.219^{-06}	1.528^{-06}	2.435^{-06}	2.659^{-06}

2.4.2 Heat Capacity and Entropy Data

Table 2.7 lists the ideal gas heat capacity and entropy values evaluated by Osmont et al. [65] based on Ab-Initio calculations.

2.5 Solubility

The aqueous solubility of CL-20 has been measured as a function of temperature by Monteil-Rivera et al. [51], and by Karakaya et al. [66]. Tables 2.8 and 2.9 list their data. The results from these two sets of data do not agree closely, and the difference between the two sets of data increased with the increase in temperature. This could be due to the analytical techniques used, the purity of the chemical, and the degree of conversion of ε-CL-20 to other phases, particularly the γ-phase. Holtz et al. [67]

Table 2.7 Ideal gas heat capacity and entropy [65]

T (K)	300	400	500	600	800	1000	1500
C _p ^o (cal mol ⁻¹ K ⁻¹)	91.1	114.2	132.6	146.8	166.1	178.1	193.4
T (K)	2000	2500	3000	3500	4000	4500	5000
C _p ^o (cal mol ⁻¹ K ⁻¹)	200.2	203.7	205.7	206.9	207.8	208.3	208.8
T (K)	300	400	500	600	800	1000	1500
S ^o (cal mol ⁻¹ K ⁻¹)	167.3	196.8	224.3	249.8	295.0	333.4	409.0
T (K)	2000	2500	3000	3500	4000	4500	5000
S ^o (cal mol ⁻¹ K ⁻¹)	465.7	510.8	548.2	580.0	607.7	632.2	654.2

Table 2.8 Aqueous solubility of CL-20 as a function of temperature [68]

Solubility of CL-20		
Temperature (°C)	(mg/L)	Mole fraction
4	2.27 (± 0.09)	9.33 10 ⁻⁸
19.5	3.11 (± 0.06)	1.41 10 ⁻⁷
25	4.33 (± 0.04)	178 10 ⁻⁷
30	5.46 (± 0.02)	2.26 10 ⁻⁷
35	6.69 (± 0.01)	2.86 10 ⁻⁷
39	8.10 (± 0.06)	3.33 10 ⁻⁷
45	11.30 (± 0.25)	4.64 10 ⁻⁷
50	14.16 (± 0.47)	5.82 10 ⁻⁷
55	17.37 (± 0.17)	7.14 10 ⁻⁷
60	23.98 (± 0.41)	9.85 10 ⁻⁷
65	32.36 (± 1.03)	1.33 10 ⁻⁶
69	39.68 (± 0.25)	1.63 10 ⁻⁶

Table 2.9 Aqueous solubility (*S*) of CL-20 as a function of temperature [68]

t (°C)	5	10	15	20	30	40	50	60
S (mg/L)	1.97	2.12	2.48	3.16	4.89	7.39	11.62	18.48

observed a transition in the solubility for CL-20 in different solvents. The solubility of CL-20 in thirteen solvents—acetone, bis(fluorodinitroethyl) formal, ethanol, ethyldinitropentanoate, ethyl acetate, ethylene glycol, FM-1 (FM-1 is a liquid explosive composed of 25% FEFO, 25% bis(dinitropropyl) formal, and 50% fluorodinitroethyl dinitropropyl formal (by mole percent), methylene chloride, nitroglycerid triacetin 75/25 (NG/TA), nitroplasticizer (NP), triethyleneglycol dinitrate, trimethylolethane tri-nitrate, and water were measured. The solubility-temperature relation for each solvent was provided by them.

The solubility data collected by Monteil-Rivera et al. [51] are shown in Table 2.9 and graphically in Fig. 2.12. During measurements, the authors found that CL-20 decomposed in non-acidified water upon contact with glass containers to give NO_2^- (2 equiv.), N_2O (2 equiv.), and HCOO^- (2 equiv.).

2.6 Decomposition and Destruction

Thermal Decomposition

Thermal decomposition of HNIW starts above 210 °C. Turcotte et al. [68] studied thermal behavior of CL-20 under various conditions using different techniques that included DSC, TG, Heat Flux Calorimetry, Accelerating Rate Calorimetry, and simultaneous TG-DTA-FTIR-MS analysis. NO_2 is the most significant product of the decomposition. Other compounds that are identified from FTIR included N_2O , CO_2 , HCOOH , HNCO , H_2O , HCN , CO and NO . The gaseous products; CO_2 , N_2O , NO_2 , HCN , NO and CO are result of secondary decomposition reactions. They also noted that the heating rate and the purge gas used during heating had no effect on the decomposition products or the mass loss, which was between 80 and 98% of the initial mass. Korsounskii et al. [70] studied the thermal decomposition characteristics along with the kinetics for HNIW. As expected, the rate of mass loss of CL-20 was dependent on temperatures and found a final mass loss of about 80% in air within 200 min in the temperature range of 183–211 °C. In comparison, HMX did not show any decomposition at 220 °C within 200 min. Based on the IR spectrum, the authors conclude that the hemolytic cleavage of the N– NO_2 bond to be the primary cause of HNIW decomposition. The effect of particle size on thermal decomposition of CL-20 has been discussed by Dong et al. [71]. They compared the decomposition steps for isothermal and non-isothermal decomposition for 40 and 230 μm particles. The 230 μm particles decomposed in two steps under non-isothermal conditions, where as it was a one step decomposition for smaller particles. The main products identified using FTIR were NO ,

N_2O , CO_2 , and a small amount of NO_2 and $\text{C}_2\text{N}_2\text{H}_2$. During isothermal decomposition, the decomposition products from larger HNIW particles at 204 °C were same as that observed in the first step of the non-isothermal decomposition.

Several researchers focused on the decomposition kinetics and developed expressions for the reaction rates. Korsounskii et al. [70] found that the solid state decomposition follows first-order kinetics and that it is an autocatalytic decomposition. The thermogravimetry analysis in a narrow temperature range of 458–477 K resulted in an activation energy of 151.7 kJ/mol and a frequency factor of $10^{13.6} \text{ s}^{-1}$. The decomposition reaction rate is represented by:

$$\frac{dx}{dt} = k_1(1 - \alpha) + k_2\alpha(1 - \alpha)$$

$$\alpha = \frac{m_0 - m}{m_0 - m_\infty}$$

where m_0 is the weight of the starting sample, m is its weight at time t and m_∞ is the weight of the sample at the end of experiment and k_1 and k_2 are given by:

$$k_1 = 10^{20.5 \pm 0.8} e^{\left(-\frac{53,400 \pm 1500}{RT}\right)}$$

$$k_2 = 10^{17.3 \pm 1.4} e^{\left(-\frac{44,700 \pm 2900}{RT}\right)}$$

Bohn [72] provides a general model for isothermal decomposition of solid energetic materials, and verified his model with data on ϵ -CL-20. Kinetic parameters and Arrhenius parameters are developed. The following expression was suggested for approximation of the HNIW decomposition during which a mass loss of 0–11% would occur.

$$ML(t, T) = O + \frac{m_C}{m_A} [1 - M_{Ar}(t, T)] \times 100\%$$

The parameter, O , stands for an offset not caused by the decomposition of compound A.

Figure 2.13 shows some of the results of this study. The solid lines in Fig. 2.13 show the model calculations, and dots represent the experimental data over a range of temperatures and time. Based on the model and experimental data Bohn concludes that the thermal decomposition of HNIW is autocatalytic.

Qasim et al. [73] carried out theoretical computations using MOPAC [Molecular Orbital PACKage] quantum mechanical and classical force field mechanics to assess the type of bond degradation in CL-20. The FTIR and UV/FTIR were used to follow the decomposition of HNIW and the data were used for theoretical calculations, and concluded that the breakage of C–N bonds to be a plausible mechanism. In addition, they computed the dipole moment and enthalpies of formation. The values of the enthalpies of formation show that the PM3 model to be better than MNDO and AM1

models [73]. Qasim et al. [73] also reviewed the research work carried out to understand structural relationships and degradation mechanisms of current and a number of emerging explosives, including nitroaromatics, cyclic and cage cyclic nitramines, and a nitrocubane. The competitive degradation mechanisms by free radical oxidative, reductive and alkali hydrolysis were studied, that included, 2,4,6-trinitrotoluene (TNT); 1,3,5-trinitrobenzene (TNB); 2,4,6-trinitrophenol (TNP or picric acid); hexahydro-1,3,5-trinitro-1,3,5-triazine (RDX); octahydro-1,3,5,7-tetranitro-1,3,5,7-tetrazocine (HMX); 2,4,6,8,10,12-hexanitro- hexa-azoisowurtzitane (CL-20); and 2,4,6,8-tetranitro1,3,5,7-tetraaza-cubane (TNTAC), and octonitrocubane (ONC).

The thermal decomposition study of CL-20 (hexanitrohexaazaisowurtzitane) using pyrolysis GC/MS was carried out mainly by electron impact (EI) mode. Chemical ionization (CI) mode was used for further confirmation of identified species. Mass spectrum of CL-20 decomposition products predominantly revealed fragments with m/z 81 and 96 corresponding to $C_4H_5N_2^+$ and $C_4H_4N_2O^+$ ions, respectively. The total ion chromatogram (TIC) of CL-20 pyrolysis shows a peak within the first 2 min due to the presence of low molecular weight gases. Peaks corresponding to several other products were also observed including the atmospheric gases. Cyanogen formation (C_2N_2 , m/z 52) observed to be enriched at the scan number 300–500. The low molecular mass range decomposition products formed by cleavage of C–N ring structure were found in majority. Additional structural information was sought by employing chemical ionization mode. The data generated during this study was instrumental in determining decomposition pathways of CL-20, and it is shown in Fig. 2.14 [76].

2.7 Hydrolysis of Hexanitrohexaazaisowurtzitane

HNIW can also be degraded through a hydrolysis reaction. Pavlov et al. [74] investigated the hydrolysis of the α , β , and ϵ polymorphs of 2,4,6,8,10,12-hexanitro-2,4,6,8,10,12-hexa azaiso-wurtzitane in dilute buffered aqueous solutions over a pH range of 4–10 and at 35, 43, 50, 58 and 65 °C, with starting concentrations of CL-20 at one half the solubility limit for the respective temperature. Figure 2.15 shows the hydrolysis rates at 50 °C at different pH values. In all cases, an overall first-order kinetic behavior was observed. The rate constants, half-lives, activation energies, and Arrhenius pre-exponential factors were determined. The latter was found to vary linearly with pH [74]. Specifically for each polymorph, the observed pseudo-first order hydrolytic rate constants at any pH and temperature in sub-solubility regions are as follows:

$$\frac{d[C_t]}{dt} = -k'[C_t]$$

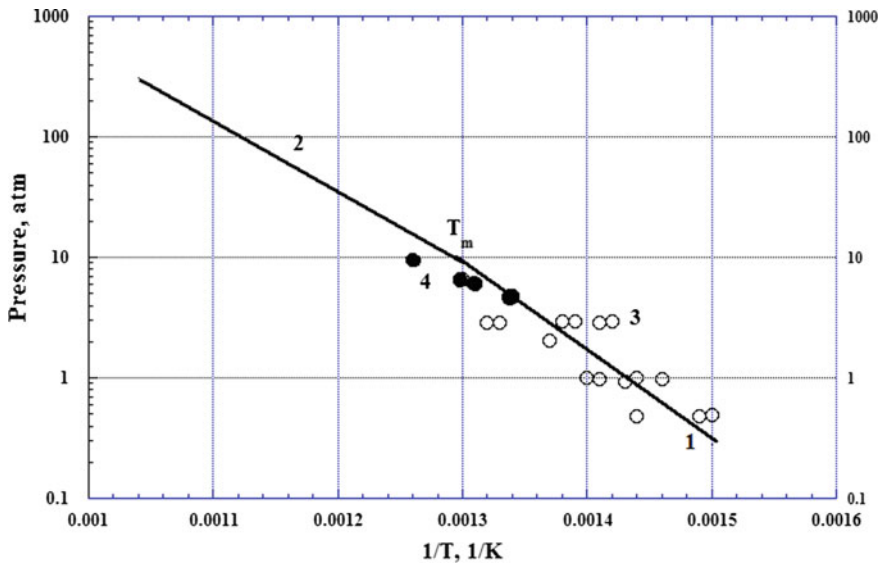


Fig. 2.11 Vapor pressure as a function of reciprocal temperature: vapor pressure above solid (1) and liquid CL-20 (2), and CL-20 surface temperatures [63]

$$k'_\alpha = (9.439 \times 10^5 pH + 6.905 \times 10^6) \exp\left(-\frac{55748}{8.314 \times T}\right)$$

$$k'_\beta = (5.085 \times 10^5 pH + 2.332 \times 10^5) \exp\left(-\frac{61530}{8.314 \times T}\right)$$

$$k'_\varepsilon = (6.662 \times 10^4 pH + 4.875 \times 10^5) \exp\left(-\frac{56276}{8.314 \times T}\right)$$

Santiago et al. [75] studied the chemical remediation of soils containing CL-20 by alkaline hydrolysis. Their study is confined to lower concentration of CL-20, shorter time periods but at higher pH values compared to the study of Pavlov et al. [74]. From their results, alkaline hydrolysis appears to be faster, and removal greater than 90% was reported.

2.8 Biodegradation

Trott et al. [77] examined CL-20 in soil microcosms to determine its biodegradability. CL-20, after incubation with a variety of soils disappeared in all microcosms except in the controls in which microbial activity had been inhibited. CL-20 was degraded most rapidly in garden soil. After 2 days of incubation, about 80% of the

initial CL-20 had disappeared. A CL-20-degrading bacterial strain, *Agrobacterium* sp. strain JS71, was isolated from enrichment cultures containing garden soil as an inoculum, succinate as a carbon source, and CL-20 as a nitrogen source. Growth experiments revealed that strain JS71 used 3 mol of nitrogen per mol of CL-20.

Jenkins et al. [60] found that the half-life of CL-20 is dependent on the soil type. The rate of loss and estimation of the half-lives of several explosives were carried out by exposing them to three test soils. The mean concentrations obtained at each time period were plotted as the $\ln(C/C_0)$ versus time (t), where C is the concentration at time t and C_0 is the initial concentration at time zero. Assuming, a first-order rate process, the half-life was determined using the following simple rate equation

$$\ln(C/C_0) = -kt$$

where k is the rate constant equal to the slope of the relationship. It may be noted that when the rate is first order, the half-life is independent of the starting concentration. Their finding is given in Table 2.10.

Crocker et al. [78] hypothesized that the biodegradation of cyclic nitramines such as CL-20 takes place by one or more of the mechanisms such as the formation of a nitramine free radical and loss of nitro functional groups, by the reduction of nitro functional groups, by direct enzymatic cleavage, by α -hydroxylation, and/or by hydride ion transfer. The intermediates formed by one or more of the pathways spontaneously decompose in water producing nitrite, nitrous oxide, formaldehyde, or formic acid as common end products. They summarize in a table the degrading bacteria and possible biochemical mechanisms for degradation of TNT, RDX, HMX, and CL-20, and show the pathways of degradation mechanism.

Both aerobic and anaerobic bacteria have been used to study the degradation of CL-20. Among the several bacteria used by the NRC Group of Canada, *Phanerochaete chrysosporium* and *Irpex lacteus* were found to degrade CL-20 [79]. Both *P. chrysosporium* and *I. lacteus* were able to remove almost all the nitramine after 25 days of incubation, and no CL-20 intermediates were detected. The proposed degradation pathway based on several publications [80, 81] by this group is shown in Fig. 2.16. They found that CL-20 transforms via an N-denitration mechanism, and putative doubly denitrated CL-20 inter-mediate and finally to the

Table 2.10 Half-life estimates (days) in three test soils [60]

Analyte	FG	CG	YTC
HMX	133	433	2310
TNAZ	<1	<1	<1
RDX	94	98	154
CL-20	69	267	144
NG	0.49	<1	<1
PETN	2.4	0.45	1.4

FG Fort Greely soil; CG Camp Guernsey soil; YTC Yakima Training Center soil

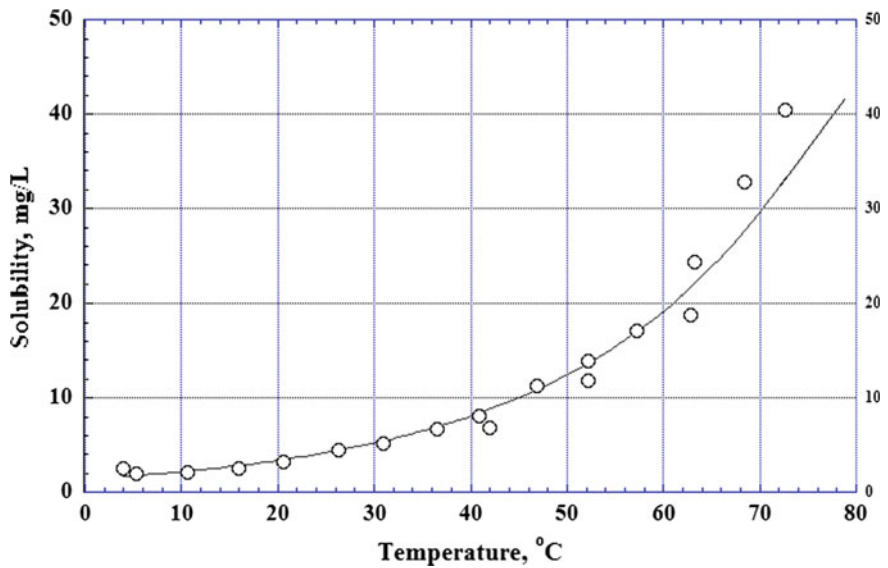


Fig. 2.12 Temperature-solubility of CL-20 in water

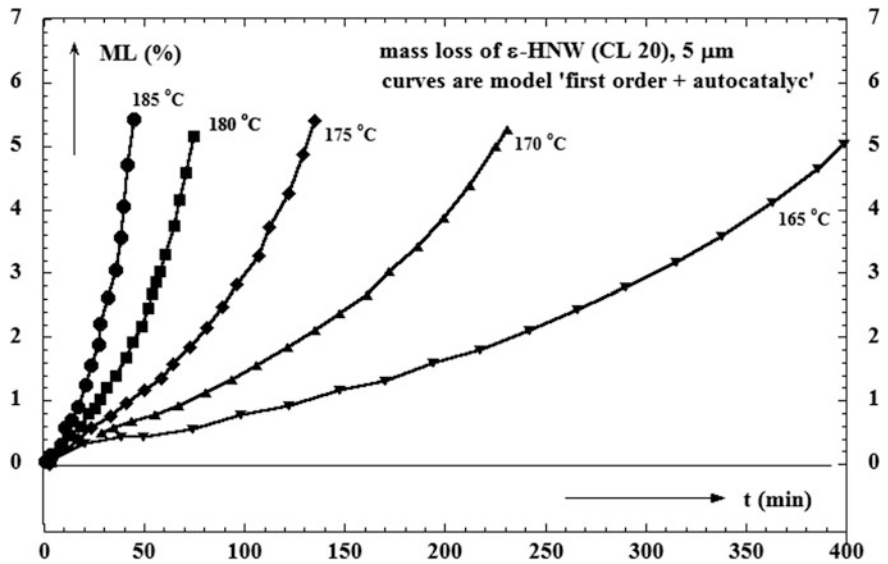


Fig. 2.13 Isothermal TGA data of ϵ -HNIW [72]

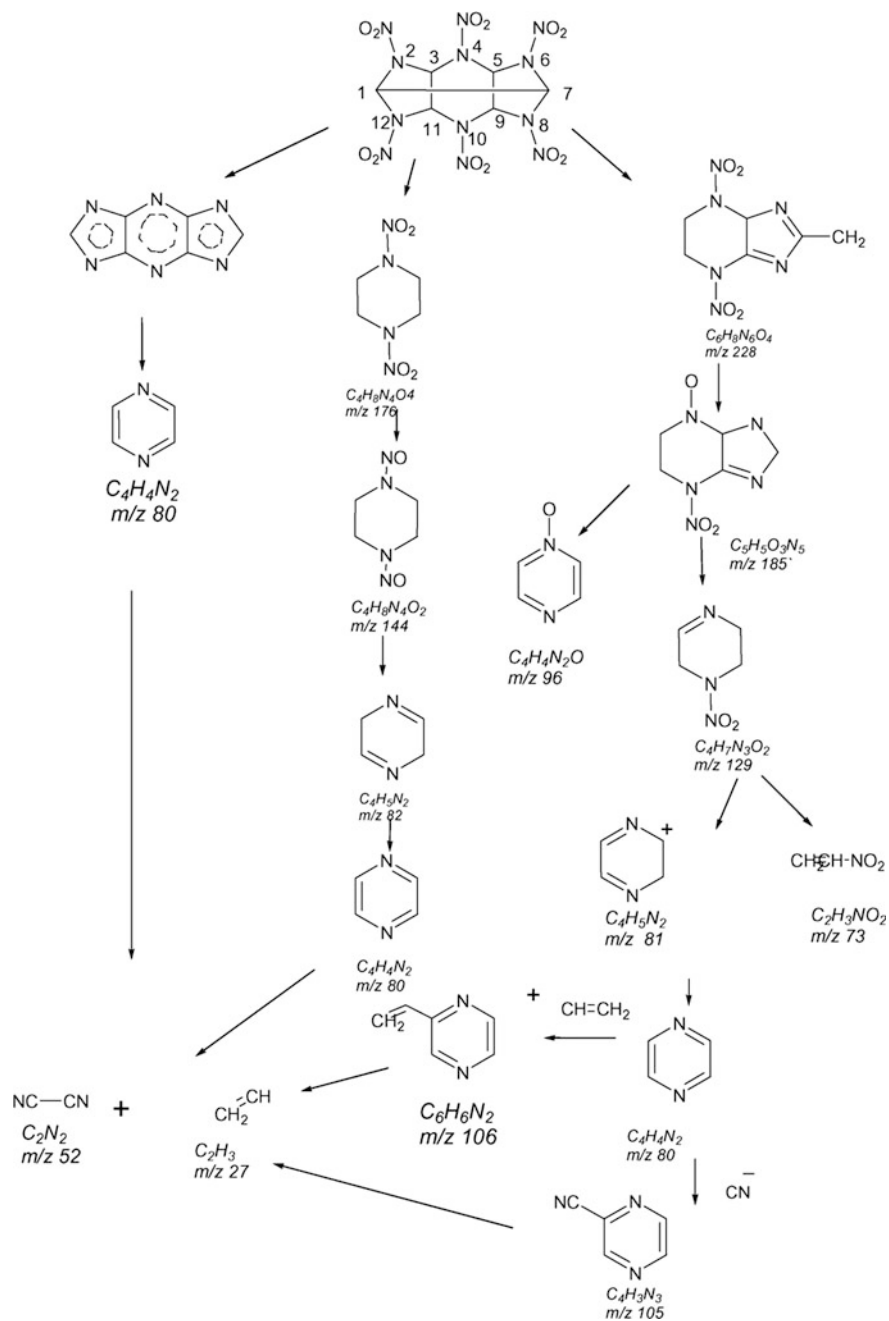


Fig. 2.14 Decomposition mechanism of CL-20 [76]

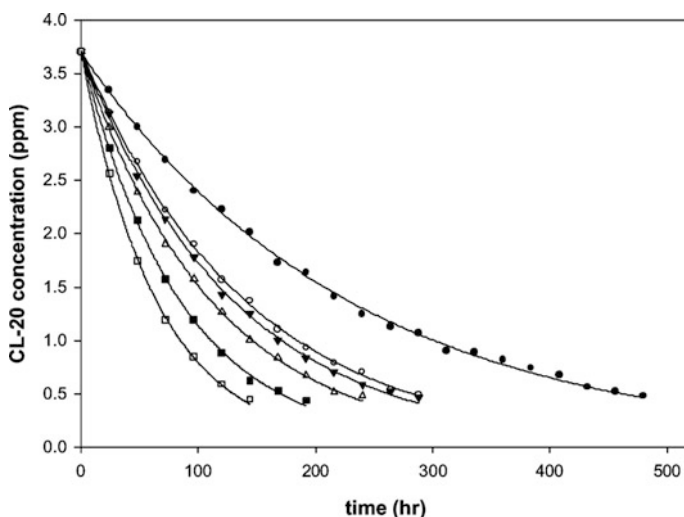


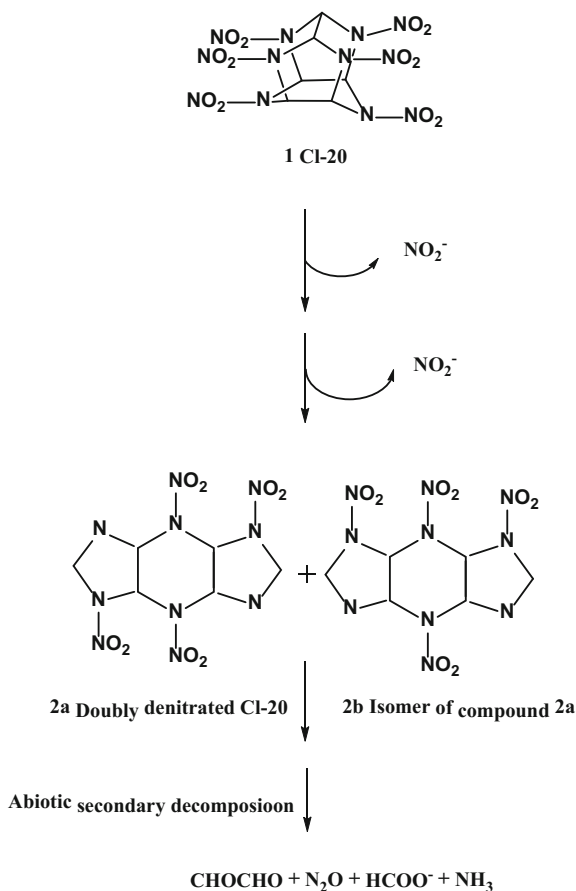
Fig. 2.15 Hydrolysis of α -CL-20 at 50 °C (●: data at pH 4; ○: data at pH 5.5; ▼: data at pH 7; Δ: data at pH 8; ■: data at pH 9; □: data at pH 10; —: exponential decay models) [74]

end products nitrous oxide (N_2O), formate (HCOO^-), ammonia (NH_3), and glyoxal (CHOCHO) as shown in Fig. 2.16 (Figs. 2.13, 2.14, and 2.15).

2.9 Spectroscopy

Kholod et al. [82] have carried out the B3LYP/6-31+G(d,p) level of theory studies to simulate IR and Raman spectra of different polymorphs of HNIW, and compared the theoretical values with experimental data of both IR and Raman spectra. They also found that the most stable conformers of CL-20, which correspond to experimentally obtained polymorphs, the pattern $\beta > \alpha$ and $\gamma > \epsilon > \zeta$ for relative stability. Table 2.11 reproduced from their paper shows the assignments for IR and Raman, and experimental values. Experimental FTIR spectrum of a standard CL-20 sample obtained by Qasim et al. [83] as well as some characteristic bands in the experimental FTIR [84] spectra. Goede et al. [85] used FT-Raman to characterize the four stable phases of CL-20. They also report reported over the region from 0–4000 cm^{-1} and assigned the most predominant Raman. They use this method for detecting polymorphic impurities in ϵ -CL-20, and the detection level for polymorphic impurities was determined to be below 2%.

Fig. 2.16 Structure of CL-20 (1) and CL-20 denitration products (2a and 2b) observed during treatment with FeO [79, 80] or with nitro-reductase [81]



2.10 Formulations and Detonation Characteristics

According to Simpson et al. [61] the explosive performance of ϵ -CL-20 is approximately 14% greater than HMX making it the most powerful explosive ever tested. They determined a number of detonation properties of CL-20 and compared with other explosives. Various detonation and morphological properties are summarized in Tables 2.12–2.17). They have also provided information on calorimetric and thermal properties, Jones-Wilkins-Lee equation of state to correlate the detonation parameters, and comparison with other explosive materials.

Table 2.11 Experimental and spectra of pure CL-20 polymorphs and the FTIR spectrum of a standard CL-20 sample [82]

ε	FTIR				CL-20	ε	Raman		
	α	β	γ	ζ			α	β	γ
		–		3038	3043 w	3048 vs	3058 s	3055 m	3062 m
				3031	3016 w	3031 m	3036 m	3045 m	3044 m
				1603	1605 s	3020 w	3028 m	3035 m	3035 w
				1568	1589 s		2924 w		
				1541	1566 s				
				1379	1381 w				
				1346					
				1332	1327 s				
				1284	1285 vs				
				1263	1265 vs				
				1229	1219 sh				
1191.7				1184		1190 m	1192 w	1188 w	1080 w
1182.5	1169.6	1178.6	1180.4		1180 w	1180 m	1170 m	1175 m	
	1168.1	1171.8							
		1154.4	1153	1161			1150 m	1155 m	1048 m
1139.2					1138 sh	1135 m		1130 w	
1125.1	1121.1		1106.1		1126 m	1125 s	1120 sh	1125 w	1020 w
1087.2	1119.8	1094.7	1080.4			1115 w			1105 m
1118.3					1088 m	1085 m	1095 vs	1090 vs	1083 m
	1094.9								
	1082								
	1078.3								
	1072.8							1060 s	
1051.6	1052.4	1052.3	1043.8	1038	1045 s	1055 vs	1054 s	1055 s	
1022.1						1010			1020 w
998.7	990.7	991.8					1000 s	1000 s	
980.9	989.2		970.6	970	980 m				
	953	959.2	958.8						
	951.7								
	949.1								
	947.7								

(continued)

Table 2.11 (continued)

		FTIR					Raman		
ε	α	β	γ	ζ	CL-20	ε	α	β	γ
944.4	945.2	944.9		946	941 s				
938.3			938.1						
913.2	904.3	907.7	909.4	904	910 sh w				
900.3			938.1						
883.8	881.7	882.9	879.2	875	883 s				
855.4	860.2	835.4	858.3		856 m	857 w	861 w	854 w	861 w
831.6	835.4		834.4	833	829 m	832 m	842 m	835 m	849 m
820.2	825.3		831.7		818 m	820 s	825 w		836 w
				800		791 w	895 w	805 w	895 w
	764.9	766.8	764.1	770	764.9			792 w	
758.2	757.7		755.8	755	756 s	755 w	762 w	763 w	762 w
751.4	751.1								
744.5	746.5	746.4	741	745	741 s				
738.2									
723.9	718	718.9	719.5		721 s				
705.1					706 sh				
					660 sh				
							283 w	284 w	287 w
						267 w			270 w

Table 2.12 Small scale safety test results

Material	Impact ^(a) (cm)	Friction ^(b) (kg)	Spark ^(c)	CRT ^(d) (cm ³ /g)
β -CL-20 ^(e)	14	6.4	no rxn	0.24
ε -CL-20 ^(f)	12–16	6.4–7.2	no rxn	0.16
ε -CL-20 ^(g)	17	6.4	no rxn	0.10
ε -CL-20 ^(h)	21	6.2	no rxn	na

^(a) 2.5 kg Type 12 tool with 35 mg pressed samples^(b) Julius-Peters-Berlin 21 friction machine. One reaction in ten tries^(c) Ten tries at 1 J with 510 R in line resistance^(d) 22 h at 120 °C under 1 atm He^(e) LLNL synthesized CL-20^(f) Aerojet synthesized CL-20. The median value is approximately 15 cm^(g) Thiokol synthesized CL-20^(h) Thiokol synthesized CL-20. Ground by NAWC, China Lake, to 3-5 pm**Table 2.13** Heats of combustion and formation [61]

Material	$\Delta H_{\text{combustmn}}$ (10 ⁶ J/mol)	$\Delta H_{\text{formation}}$ (10 ³ J/mol)
β -CL-20	−3.649	+431.0 ± 13
ε -CL-20	−3.596	+377.4 ± 13

Table 2.14 Calorimetric heat of detonation of CL-20 [61]

Materials	ρ (g/cm ³)	J/g ^(a)	J/cm ³	J/cm ³ at TMD ^(b)
ε -CL-20 experimental	1.96	6.234 \pm 63	12,219 \pm 123	12,717 \pm 129
ε -CL-20 experimental estimated from products	1.96	6.029 \pm 146	11,817 \pm 286	123,013 \pm 298

Table 2.15 Performance characteristics of explosive components [86]

Substance	ΔH_f (kcal/kg)	Q (g/cm ³)	D _{calc} (m/s)	P _{cj} (GPa)	ΔE at V/V ₉ = 6.5 (kJ/cm ³)	V _{gas} at 1 bar (cm ³ /g)
TNT	−70.5	1.654	6881	19.53	−5.53	738
RDX	72.0	1.816	8977	35.14	−8.91	903
HMX	60.5	1.910	9520	39.63	−9.57	886
PETN	−407.4	1.778	8564	31.39	−8.43	852
TATB	−129.38	1.937	8114	31.15	−6.94	737
HNS	41.53	1.745	7241	23.40	−6.30	709
NTO	−237.8	1.930	8558	31.12	−6.63	768
TNAZ	45.29	1.840	9006	36.37	−9.39	877
CL-20	220.0	2.044	10065	48.23	−11.22	827

Table 2.16 Insensitive munitions properties of and new energetic materials [86]

Substance	Friction sensitivity (N)	Impact sensitivity (Nm)	Deflagration point (°C)
TNT	353	15	300
RDX	120	7.4	230
HMX	120	7.4	287
CL-20	54	4	228

The materials data sheet from Société nationale des poudres et explosifs, France (SNPE) lists the following properties for CL-20:

Deflagration temperate: 220–225 °C

Decomposition temperate: 213 °C

Maximum Decomposition temperate: 249 °C

Heat of Decomposition: 2300 J/g

Detonation velocity: 9650 m/s (experimental value)

Vacuum test, 193 h at 100 °C: 0.4 cm³/g

2.11 CL-20 Based Formulations

Various CL-20 based formulations are available for use in both propellants and explosives. A large number of CL-20-based plastic bonded explosives (PBXs) are developed to enhance the explosive powers, and the burning rate in the case of propellants. Nair et al. [87] carried out thermal and sensitivity studies on CL-20

Table 2.17 Properties of CL-20 Polymorphs [86]

Property	γ -CL-20	α -CL-20	β -CL-20	ε -CL-20	HMX
Density (g/cm ³)	1.92	1.97	1.99	2.04	1.91
Detonation velocity (m/s)	9380	9380	9380	9660	9100
Phase transition temperate (°C)	260	170	163	177	280

Table 2.18 Density and velocity of detonation of selected CL-20-based PBXs [87–90]

Composition	Density (g/cm ³)	Detonation velocity [mm/(μ sec)]
96% CL-20; 1% Hy Temp; 3% DOA	1.901	9.018
96% HMX; 1% Hy Temp; 3% DOA	1.792	8.748
RX-39-AA&AB: 95.5–95.8% CL-20; estane	1.942 \pm 0.001	9.208
PBXC-19: 95% CL-20; EVA	1.896 \pm 0.002	9.083
PATHX-1: 88–95% CL-20; estane	1.868–1.944	8.89–9.37
PATHX-2: 92–95% CL-20; estane	1.869–1.923	8.85–9.22
PATHX-3: 85–94% CL-20; estane	1.871–1.958	8.91–9.50
LX-19: 95% CL-20; estane	1.959	9.44
LX-14: 95% HMX; estane	1.835	8.79
PBXCLT-1: 49–70% CL-20; 48–27% energetic material HNJ and 3% polymeric binder PVB	1.906	8.384–9.102
PBXCL-1: 97% CL-20; 3% PVB	1.921	9.102
66.8–72.1% CL-20; HTPB	1.648–1.710	8.325–8.470
66.8–72.1% HMX; HTPB	1.575–1.618	8.030–8.107
32% CL-20; 48% TEX; 20% HTPB	1.595	
32% HMX; 48% TEX; 20% HTPB	1.560	

coated with several polymers—Ethylene vinyl acetate (EVA), copolymer of polybutylene terephthalate polyether glycol (hytel), polyurethane-ester-MDI (Estane), hexafluoropropylene vinylidene fluoride copolymer (Viton) and polyurethane (PU). Their results are given in Table 2.18 [87–90].

As shown in Table 2.18, CL-20 based formulations have 12–15% higher velocity of detonation compared to the corresponding HMX based formulations. CL-20 is also found to be a superior alternative to RDX and HMX for applications in low signature rocket propellants. CL-20 based propellants showed a 35–110% higher burning rates than those of HMX-based propellants. Golfier et al. [91] noted that the Isp of CL-20–glycidyl azide polymer (GAP) propellants is 251 s, compared to 242 s for the corresponding RDX-based propellant.

Li and Brill [92] discuss nanostructured energetic compounds of CL-20. They found that the cryogel method enabled them to load up to 90% of CL-20 (by mass) in energetic polymer matrices composed of single precursors of GAP polyol, NC, and THMNM and their mixed precursors. One of the objectives for development of

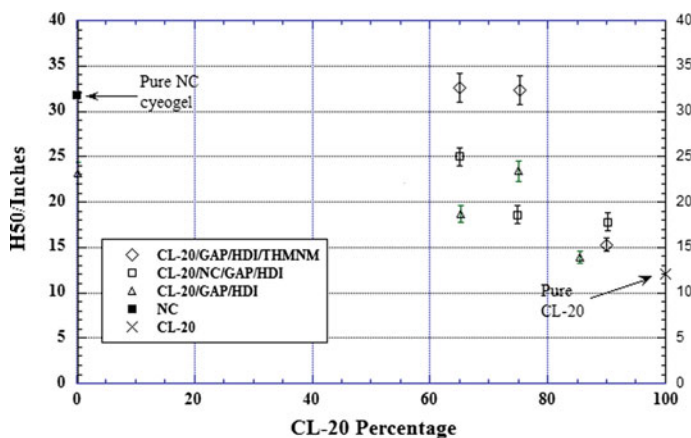


Fig. 2.17 Drop weight impact test data of energetic polymer gels and composite energetic gels CL-20 in the 50–70% by weight range appear to have a notable reduction in sensitivity [92]

Table 2.19 Burning rates of CL-20-incorporating rocket propellants [69, 91–93]

Composition	Burning rate (mm/sec)	n
60% CL-20; 40% PGA	11.5–23 (7–15 MPa)	0.92
60% HMX; 40% PGA	6–11 (7–15 MPa)	0.89
60% CL-20; 40% GAP 1	3.4–27.2 (7–15 MPa)	0.94
60% HMX; 40% GAP	7.2–13.6 (7–15 MPa)	0.91
60% CL-20; 40% GAP	20.0–32.4	0.48
(catalyzed)	(7–20 MPa)	
60% RDX; 40% GAP	14.6–21.4	0.37
(catalyzed)	(7–20 MPa)	
70% CL-20; 20% GAP;	15	0.57
10% BDNPF/A	(7 MPa)	

Note n is the exponent in the power law of the burning rate, PGA is polyglycol adipate, and GAP is a glycidyl azide polymer

this product was to reduce the sensitivity of the formulations. The sensitivity determine by the drop test is shown in Fig. 2.17 (Table 2.19).

Mueller [94] has studied several formulations of CL-20 and RDX with nitrocellulose, BDNPA/F, EPX, and a stabilizer, and compared the properties of these two explosives. Mueller has presented thermodynamic and chemical stability data along with 40-mm gun simulation data as a function of temperature.

Besides using CL-20 as an explosive, it is also used as a propellant. It is being tested as an alternative to ammonium perchlorate in missile and space applications. Golfier et al. [89] found that CL-20 propellants offer 7% superior I_{sp} (251 s) compared to RDX-based formulations. Weiser et al. [95] found that the CL-20/glycidylazide polymer-(GAP) propellants exhibit burning rates twice those of

HMX/GAP propellants. Attempts have been made to ballistically modify CL-20 formulations, but specific information about the modifiers is not available. Nair et al. [96] have studied CL-20 based composites as double-based propellants. With corporate 17.5% aluminum based on their theoretical evaluation of I_{sp} . In another paper, Thepenier and Fanblanc [97] compare the characteristics of several compounds and show the superiority of CL-20 with respect to density, enthalpy of formation, and oxygen balance. In addition this paper provides information on a wide variety of fields from new raw materials (energetic binders, plasticizers, oxidizers) through new propellants and new processes to new tools for designing grains. Unlike many other propellants, the CL-20 propellant exhaust is free of lead, acids, and aluminum oxide emissions. The absence of halogens like in ammonium perchlorate makes CL-20 products of combustion more environmentally friendly.

2.12 Toxicity

Kuperman et al. [98, 99] have reported the Enchytraeid Reproduction Test, and found that toxicities for *E. crypticus* adult survival and juvenile production significantly increased in weathered and aged treatments compared with toxicity in freshly amended soil, based on 95% confidence intervals. The EC50 and EC20 values for juvenile production were 0.3 and 0.1 mg kg⁻¹ for CL-20 freshly amended into soil, and 0.1 and 0.035 mg kg⁻¹, respectively, for weathered and aged CL-20 treatments.

2.13 Conclusion

CL-20 has attracted a great deal of attention in the recent years as a powerful insensitive explosive. Current literature search revealed that several countries are working on this explosive mainly on the synthesis, scale-up, and cost reduction. There is little work on properties, detection, toxicity, and remediation of contaminated sites should this be made in large quantities.

References

1. Nielsen AT (1997) Caged polynitramine compound. US Patent 5693794
2. USA Navy Manteca (2004) Report of 2003. Dept of Navy, Fiscal Year 2003 Rpt
3. Nielsen AT, Nissan RA, Vanderah DJ, Coon CL, Gilardi RD, George CF, Lippen-Anderson JF (1990) Polyazapolycyclics by condensation of aldehydes with amines 2 Formation of 2,4,6,8,10,12-Hexabenzyl-2,4,6,8,10,12-hexaazatetra - cyclo [55000] dodecanes from glyoxal and benzylamines. J Org Chem 55(5):1459–1466

4. Crampton MR, Hamid J, Millar R, Ferguson G (1993) Studies of the synthesis, protonation and decomposition of 2,4,6,8,10,12-hexabenzyl-2,4,6,8,10,12-hexaazatetracyclo[55005,903,11]dodecane (HBIW). *J Chem Soc Perkin Trans 2*(5):923–929
5. Edwards WW, Wardle RB (1998) Process for making 2,4,6, 8,10,12- hexanitro- 2,4,6,8,10, 12-hexa azatetracyclo 550 0 5,9 0 3,11] –dodecane. EP 1153025 A2 (WO2000052011A2), US Patent 5739325
6. Kodama T (1994) Preparation of hexakis (trimethylsilylethylcarbamyl) hexaazaisowurtzitane. JP06321962A
7. Kodama T, Tojo M, Ikeda M (1996) Acylated hexaazaisowurtzitane derivatives and process for producing the same. WO9623792A1
8. Ou Y-x, Xu Y-j, Liu L-h, Zheng F-p, Wang C, Chen J-t (1999) Comparison of acetonitrile process with ethanol process for synthesis of hexabenzylhexaazaisowurtzitane. *Hanneng Cailiao* 7(4):152–155
9. Ou Y, Xu Y, Chen B, Liu L, Wang C (1999) Synthesis of hexanitrohexaazaisowurtzitane from tetraacetyldiformylhexaazaisowurtzitane. *Proc Int Pyrotech Semin* 26th:406–411
10. Ou Y, Meng Z, Liu J (2007) Advance in high energy density compound CL-20-developments of synthesis route and production technologies of CL-20. *Huagong Jinzhan* 26 (6):762–768
11. Sysolyatin SV, Lobanova AA, Chernikova YT, Sakovich GV (2005) Methods of synthesis and properties of hexanitrohexaazaisowurtzitane. *Russ Chem Rev* 74(8):757–764. doi:[10.1070/RC2005v074n08ABEH001179](https://doi.org/10.1070/RC2005v074n08ABEH001179)
12. Wang C, Ou Y-X, Chen B-R (2000) One pot synthesis of hexabenzylhexaazaisowurtzitane. *Beijing LigongDaxueXuebao* 20(4):521–523
13. Nielsen AT, Chafin AP, Christian SL, Moore DW, Nadler MP, Nissan RA, Vanderah DJ (1998) Synthesis of polyazapolycyclic caged polynitramines. *Tetrahedron* 54(39):11793–11812. doi:[10.1016/S0040-4020\(98\)83040-8](https://doi.org/10.1016/S0040-4020(98)83040-8)
14. Larson SL, Felt DR, Davis JL, Escalon L (2002) Analysis of CL-20 in environmental matrices: water and soil. *J Chromatogr Sci* 40(4):201–206. doi:[10.1093/chromsci/404201](https://doi.org/10.1093/chromsci/404201)
15. Hamilton RS, Sanderson AJ, Wardle RB, Warner KF (2000) Studies of the crystallization of CL-20. International Annual Conference of ICT [Institut ChemischeTechnologie], 31st (Energetic Materials), 21/1–21/8
16. Bellamy AJ (1995) Reductive debenzylation of hexabenzylhexaazaisowurtzitane. *Tetrahedron* 51(16):4711–4722
17. Surapaneni R, Damavarapu R, Kumar RA, Dave PR (2000) Process improvements in CL-20 manufacture. International Annual Conference of ICT, 31st (Energetic Materials), 108/1–108/4
18. Qian H, Ye Z-W, Lv C-X (2007) Efficient and facile synthesis of hexanitrohexaazaisowurtzitane (HNIW) for high energetic materials. *Lett Org Chem* 4(7):482–485
19. Qian H, Chunxu LV, Zhiwen YE (2008) Synthesis of CL-20 by clean nitrating agent dinitrogen pentoxide. *J Indian Chem Soc* 85(4):434–439
20. Qian H, Ye Z-W, Lu C-X (2008) Synthesis of CL-20 via nitration and nitrolysis of 2,6,8,12-tetraacety 1-2,4,6,8,10,12-hexaazaisowurtzitane with N_2O_5/HNO_3 . *Yingyong Huaxue* 25(3):378–380
21. Song ZW, Yan QL, Li XJ, Qi XF, Lim M (2010) Crystal transition of CL-20 in different solvents. *Chin J Energ Mater* 6:648–653
22. Gore GM, Sivabalan R, Nair UR, Saikia A, Venugopalan S, Gandhe BR (2007) Synthesis of CL-20: By oxidative debenzylation with cerium (IV) ammonium nitrate (CAN). *Indian J Chem, Sect B: Org Chem Incl Med Chem* 46B(3):505–508
23. Kawabe S, Miya H, Kodama T, Miyake N (2007) Process for the preparation of 1,3,5,7-tetranitro-1,3,5,7-tetraazacyclooctane. US 6297372 B1, EP 0547735
24. Cagnon G, Eck G, Herve G, Jacob G (2007) Method for making new polycyclic polyamides as precursors for energetic polycyclic polynitramine oxidizers. US Patent 7279572

25. Latypov NV, Wellmar U, Goede P, Bellamy AJ (2000) Synthesis and Scale-Up of 2,4,6,8,10,12-Hexanitro-2,4,6,8,10,12-hexaazaisowurtzitane from 2,6,8,12-Tetraacetyl-4,10-dibenzyl-2,4,6,8,10,12-hexaazaisowurtzitane (HNIW, CL-20). *Org Proc Res Dev* 4(3):156–158
26. Pang S-P, Yu Y-Z, X-Q Zhao () A novel synthetic route to hexanitrohexa- azaisowurtzitane. *Propellants, Explosives, Pyrotechnics* 30(6):442–444
27. Chapman RD, Hollins RA (2008) Benzylamine-Free, heavy-metal-free synthesis of CL-20 via hexa(1-propenyl)hexaazaisowurtzitane. *J Energ Mater* 26(4):246–273
28. Herve G, Jacob G, Gallo R (2006) Preparation and structure of novel hexaazaisowurtzitane cages. *Chem Eur J* 12(12):3339–3344
29. Mandal AK, Pant CS, Kasar SM, Soman T (2009) Process Optimization for Synthesis of CL-20. *J Energ Mater* 27(4):231–246. doi:[10.1080/07370650902732956](https://doi.org/10.1080/07370650902732956)
30. Lu L, Xu B, Ma Z, Yue H, Mu W, Ou Y (2007) New method for synthesis and crystallizing of HNIW in nitric acid. In: Huang P, Wang Y, Li S (eds) 2007 Science Press, Proc Intl Autumn Seminar on Propellants, Explosives and Pyrotechnics, 7th, Xi'an, China, Oct 23–26, pp 64–65
31. Wang J, Li J, An C, Hou C, Xu W, Li X (2012) Study on ultrasound- and spray-assisted precipitation of CL-20. *Propellants, Explos, Pyrotech* 37(6):670–675
32. van der Heijden AEDM, Bouma RHB (2004) Crystallization and characterization of RDX, HMX, and CL-20. *Cryst Growth Des* 4(5):999–1007
33. Bellamy AJ (2003) A simple method for the purification of crude hexanitrohexaazaisowurtzitane (HNIW or CL20). *Propellants, Explos, Pyrotech* 28(3):145–152
34. Degirmenbasi N, Peralta-Inga Z, Olgun U, Gocmez H, Kalyon DM (2006) Recrystallization of CL-20 and HNX from solution for rigorous control of the polymorph type: part II, experimental studies. *J Energ Mater* 24(2):103–139. doi:[10.1080/07370650600672090](https://doi.org/10.1080/07370650600672090)
35. Agrawal JP (2011) *High Energy Materials*. Wiley, Weinheim, Germany
36. Nair UR, Sivabalan R, Gore GM, Geetha M, Asthana SN, Singh H (2005) Hexanitrohexaazaisowurtzitane (CL-20) and CL-20-based formulations (Review). *Combust Explosion Shock Waves* 41:121–132
37. Chapman RD, Hollins RA, Groshens TJ, Nissan DA (2006) Benzylamine-Free, heavy-metal-free synthesis of CL-20. SERDP seed Proect WP-1518
38. Jin S, Shu Q, Chen S, Shi Y (2007) Preparation of e-HNIW by a one-pot method in concentrated nitric acid from tetraacetylformylhexaazaisowurtzitane. *Propellants, Explos, Pyrotech* 32(6):468–471
39. Duddu R, Dave PR (1999) Processes and Compositions for Nitration of N-Substituted Isowurtzitane Compounds. Paten WO9957104, USA
40. Wardle RB, Hinshaw JC (2000) Synthesis and reactions of hexaazaisowurtzitane-type compounds in synthesis of hexanitrohexaazaisowurtzitane (HNIW) explosive. In: Cordant Technologies Inc, USA, Division of US Ser No 292 028, pp 8
41. Russell TP, Miller PJ, Piermarini GJ, Block S (1992) High-pressure phase transition in γ -hexanitrohexaazaisowurtzitane. *J Phys Chem* 96(13):5509–5512
42. Ciezak JA, Jenkins TA, Liu Z (2007) Evidence for a high-pressure phase transition of ε -2,4,6,8,10,12-hexanitrohexaazaisowurtzitane (CL-20) using vibrational spectroscopy. *Propellants, Explos, Pyrotech* 32(6):472–477. doi:[10.1002/prep200700209](https://doi.org/10.1002/prep200700209)
43. Gump JC, Peiris SM (2008) Phase transitions and isothermal equations of state of epsilon hexanitrohexaazaisowurtzitane (CL-20). *J Appl Phys* 104(8):083509/1–083509/5. doi:[10.1063/1.2990066](https://doi.org/10.1063/1.2990066)
44. Turcotte R, Vachon M, Kwok QSM, Wang R, Jones DEG (2005) Thermal study of HNIW (CL-20). *Thermochim Acta* 433:105–115
45. Ghosh M, Venkatesan V, Sikder AK, Sikder N (2012) Preparation and characterisation of ε -CL-20 by solvent evaporation and precipitation methods. *Def Sci J* 62(6):390–398
46. Meents A, Dittrich B, Johnas SKJ, Thome V, Weckert EF (2008) Charge-density studies of energetic materials: CL-20 and FOX-7. *Acta Crystallogr B* 64(Pt 1):9–42
47. Chen H, Chen S, Li L, Jin S (2008) Quantitative determination of e-phase in polymorphic HNIW using diffraction patterns. *Propellants, Explos, Pyrotech* 33:467–471

48. Cabalo JB, Sausa RC (2005) Explosive residue detection by laser surface photo-fragmentation–fragment detection spectroscopy: II *In Situ* and Real-time Monitoring of RDX, HMX, CL20, and TNT, by an Improved ion probe. Report ARL-TR-3478
49. Larson SL, felt DR, Escalon L, JD Davis, Hansen LD (2001) Analysis of CL-20 in environmental matrices water and soil. ERDC/EL TR-01-21
50. Liu Y, Chen S, Luo S (2000) HPLC method for analysis of CL-20 in explosive mixture. *Huaxue Yanjiu Yu Yingyong* 12(4):446–448
51. Monteil-Rivera F, Paquet L, Deschamps S, Balakrishnan VK, Beaulieu C, Hawari J (2004) Physico-chemical measurements of CL-20 for environmental applications Comparison with RDX and HMX. *J Chromatogr A* 1025(1):125–132. doi:[10.1016/j.chroma.2003.08.060](https://doi.org/10.1016/j.chroma.2003.08.060)
52. Anthony JS, Davis EA, Haley MV, Kolakowski JE, Kurnas CW, Phillips CT, Simini M, Kuperman RG, Checkai RT (2004) HPLC determination of hexanitrohexaazaisowurtzitane (CL 20) in soil and aqueous matrices. US Army Res Dev Eng Command Edgewood chem Bio Center, ECBE-TR, p 403
53. Makarov A, LoBrutto R, Christodoulatos C, Jerkovich A (2009) The use of ultra high-performance liquid chromatography for studying hydrolysis kinetics of CL-20 and related energetic compounds. *J Hazard Mater* 162(2–3):1034–1040. doi:[10.1016/j.jhazmat.2008.05.157](https://doi.org/10.1016/j.jhazmat.2008.05.157)
54. Oehrlé SA (1994) Analysis of CL-20 and TNAZ in the presence of other nitroaromatic and nitramine explosives using HPLC with photodiode array (PDA) detection. *J Energ Mater* 12 (4):22–211. doi:[10.1080/07370659408018651](https://doi.org/10.1080/07370659408018651)
55. Persson B, Ostmark H, Bergman H (1997) An HPLC method for analysis of HNIW and TNAZ in an explosive mixture. *Propellants, Explos, Pyrotech* 22(4):238–239
56. Agilent Technology, LC/MS Application Note, April 2004
57. Toghiani RK, Toghiani H, Maloney SW, Boddu VM (2008) Prediction of physicochemical properties of energetic materials. *Fluid Phase Equilib* 264:86–92
58. Qasim MM, Furey J, Fredrickson HL, Szecsody J, McGrath C, Bajpai R (2004) Semiempirical predictions of chemical degradation reaction mechanisms of CL-20 as related to molecular structure. *Struct Chem* 15(5):493–499. doi:[10.1023/B:STUC.0000037907.27898.f5](https://doi.org/10.1023/B:STUC.0000037907.27898.f5)
59. Zeman S, Jalovy Z (2000) Heats of fusion of polynitro derivatives of polyazaisowurtzitane. *Thermochim Acta* 345(1):31–38
60. Jenkins TF, Bartolini C, Ranney TA (2003) Stability of CL-20, TNAZ, HMX, RDX, NG, and PETN in moist, unsaturated soil. ERDC/CRREL TR-03-7
61. Simpson RL, Urtiew PA, Ornellas DL, Moody GL, Scribner KJ, Hoffmann DM (1997) CL-20 performance exceeds that of HMX and its sensitivity is moderate. *Propellants, Explos, Pyrotech* 22(5):249–255
62. Greenlief CM, Ghosh TK, Viswanath DS, Boddu VM (2010) Vapor Pressure of Hexanitrohexaazaisowurtzitane (HNIW, CL-20). Report to Leonard Wood Institute, LWI-101.1, MO, USA
63. Sinditskii VP, Egorshv VY, Berezin MV, Serushkin VV, Milekhin YM, Gusev SA, Matveev AA (2003) Combustion characteristics of the high-energy cage hexanitrohexaazaisowurtzitane nitramine. *Khim Fiz* 22(7):69–74
64. Boddu VM, Maloney SW, Toghiani RK, Toghiani H (2010) Prediction of physicochemical properties of energetic materials for identification of treatment technologies for waste streams. U.S. Army Engineer Research and Development Center, ERDC/CERL TR-10-27
65. Osmont A, Catoire L, Gökalp I, Yang V (2007) Ab initio quantum chemical predictions of enthalpies of formation, heat capacities, and entropies of gas-phase energetic compounds. *Combust Flame* 151:262–273
66. Karakaya P, Sidhoum M, Christodoulatos C, Nicolich S, Balas W (2005) Aqueous solubility and alkaline hydrolysis of the novel high explosive hexanitrohexaazaisowurtzitane (CL-20). *J Hazard Mater* 120(1–3):183–191
67. von Holtz E, Ornellas D, Foltz MF, Clarkson JE (1994) The solubility of ϵ -CL-20 in selected materials. *Propellants, Explos, Pyrotech* 19:206–212

68. Turcotte R, Vachon M, Kwok QSM, Wang R, Jones DEG (2005) Thermal study of HNIW (CL-20). *Thermochim Acta* 433(1–2):105–115
69. Highsmith T, Johnston H (2004) Continuous process for preparing alkoxy nitroarenes. ALLIANT TECHSYSTEMS INC., MINNESOTA, US 10/338,767, USA
70. Korsounskii BL, Nedel'ko VV, Chuk anov NV, Larikova TS, Volk F (2000) Kinetics of thermal decomposition of hexanitrohexaazaisowurtzitane, *Russ Chem Bull* 49:812–817
71. Ding T, Yang H, Zhang Y (2013) Thermal decomposition of CL-20/RDX mixed system. *Huaxue Tuijinji Yu Gaofenzi Cailiao* 11(6):84–86
72. Bohn MA (2002) Kinetic description of mass loss data for the assessment of stability, compatibility and aging of energetic components and formulations exemplified with ϵ -CL20. *Propellants, Explos, Pyrotech* 27(3):125–135
73. Qasim MM, Moore B, Taylor L, Honea P, Gorb L, Leszczynski J (2007) Structural characteristics and reactivity relationships of nitroaromatic and nitramine explosives—a review of our computational chemistry and spectroscopic research. *Int J Mol Sci* 8:1234–1264
74. Pavlov J, Christodoulatos C, Sidhoum M, Nicolich S, Balas W, Koutsospyros A (2007) Hydrolysis of hexanitrohexaazaisowurtzitane (CL-20). *J Energ Mater* 25(1):1–18
75. Santiago L, Felt DR, Davis JL (2007) Chemical remediation of an ordnance-related compound: the alkaline hydrolysis of CL-20. ERDC/EL TR-07-18 Report
76. Naik NH, Gore GM, Gandhe BR, Sikder AK (2008) Studies on thermal decomposition mechanism of CL-20 by pyrolysis gas chromatography-mass spectrometry (Py-GC/MS). *J Hazard Mater* 159(2–3):5–630
77. Trott S, Nishino SF, Hawari J, Spain JC (2003) Biodegradation of the nitramine explosive CL-20. *Appl Environ Microbiol* 69(3):1871–1874
78. Crocker FH, Indest KJ, Fredrickson HL (2006) Biodegradation of the cyclic nitramine explosives RDX, HMX, and CL-20. *Appl Microbiol Biotechnol* 73(2):274–290; Fournier D, Monteil-Rivera F, Halasz A, Bhatt M, Hawari J (2006) Degradation of CL-20 by white-rot fungi *Chemosphere* 63(1):175–181
79. Balakrishnan VK, Monteil-Rivera F, Gautier MA, Hawari J (2004) Sorption and stability of the polycyclic nitramine explosive CL-20 in soil. *J Environ Qual* 33(4):1362–1368
80. Balakrishnan VK, Monteil-Rivera F, Halasz A, Corbeau A, Hawari J (2004) Decomposition of the Polycyclic Nitramine Explosive, CL-20, by Fe0. *Environ Sci Technol* 38(24):6861–6866
81. Bhushan B, Paquet L, Spain JC, Hawari J (2003) Biotransformation of 2,4,6,8,10,12-hexanitro-2,4,6,8,10,12-hexaazaisowurtzitane (CL-20) by denitrifying *Pseudomonas* sp strain FA1. *Appl Environ Microbiol* 69(9):5216–5221
82. Kholod Y, Okovytyy S, Kuramshina G, Qasim M, Gorb L, Leszczynski J (2007) An analysis of stable forms of CL-20: a DFT study of conformational transitions, infrared and Raman spectra. *J Mol Struct* 843(1–3):14–25
83. Qasim M, Fredrickson H, Honea P, Furey J, Leszczynski J, Okovytyy S, Szecsody J, Kholod Y (2005) Prediction of CL-20 chemical degradation pathways, theoretical and experimental evidence for dependence on competing modes of reaction. *SAR QSAR Environ Res* 16:495–515
84. Foltz MF (1994) Thermal stability of ϵ -hexanitrohexaazaisowurtzitane in an Estane formulation. *Propellants, Explos, Pyrotech* 19(2):63–69
85. Goede P, Latypov NV, Oestmark H (2004) Fourier transform Raman Spectroscopy of the four crystallographic phases of α , β , γ and ϵ 2,4,6,8,10,12-hexanitro-2,4,6,8,10,12-hexaazatetracyclo[55005,903,11]dodecane (HNIW, CL-20). *Propellants, Explos, Pyrotech* 29(4):205–208
86. Ulrich TF (2005) *Energetic materials: particle processing and characterization*. Wiley, New York
87. Nair UR, Gore GM, Sivabalan R, Satpute RS, Asthana SN, Singh H (2004) Studies on polymer coated CL-20-the most powerful explosive *J Polym Mater* 21(4):377–382

88. Nair UR, Sivabalan R, Gore GM, Dudek K, Marecek P, Vavra P (2000) Laboratory testing of HNIW mixtures. *Proc. 31st Int Conf ICT, Karlsruhe*, June 27–30 (2000), pp 110/1–110/6
89. Mezger MJ, Nicholich SM, Geiss DA et al (1999) Performance and hazard characterization of CL-20 formulations. In: *Proceedings of 30th International Annual Conference of ICT, Karlsruhe*, June 29–July 2 (1999), pp. 4/1–4/14
90. Tian Y, Xu R, Zhou Y, Nie F (2001) Study on formulation of CL-20. In: *Proceedings of 4th International Autumn Seminar on Propellants, Explos, Pyrotech Shaoxing, China*, pp 43–47
91. Golfier M, Graindorge H, Longevialle Y, Mace H (1998) New energetic molecules and their applications in the energetic materials. In: *Proceedings of 29th International Annual Conf. of ICT, Karlsruhe*, 30 June–3 July 1998, pp 3/1–3/17
92. Li J, Brill TB (2006) Nanostructured energetic composites of CL-20 and binders synthesized by sol gel methods. *Propellants, Explos, Pyrotech* 31:61–69
93. Wagstaff DC (2002) Desensitization of energetic materials by energetic plasticizer, *Brit. UK Pat. Appl GB 2374867 A1*, 30 October 2002
94. Mueller D (1999) New gun propellant with CL-20. *Propellants, Explos, Pyrotech* 24(3):176–181. doi:[10.1002/\(SICI\)1521-4087\(199906\)24:03<176::AID-PREP176>3.0.CO;2-4](https://doi.org/10.1002/(SICI)1521-4087(199906)24:03<176::AID-PREP176>3.0.CO;2-4)
95. Weiser V, Eisenreich N, Eckl W, Eisele S, Menke K (2000) Burning behavior of CL-20/GAP and HMX/GAP rocket propellants. In: *International Annual Conference on ICT 31st (Energetic Materials)*, pp 144/141–144/146
96. Nair UR, Gore GM, Sivabalan R, Divekar CN, Asthana SN, Singh H (2004) Studies on advanced CL-20-based composite modified double-base propellants. *J Propul Power* 20 (5):952–955; Thepenier J, Fanblanc G (2001) *Acta Astronautica*, 38:245
97. Thepenier J, Fanblanc G (2001) Advanced technologies available for future solid propellant grains. *Acta Astronautica* 48(5–12):245–255
98. Kuperman RG, Checkai RT, Simini M, Phillips CT, Anthony JS, Kolakowski JE, Kumas CW, Davis EA (2006) U S Army Research, Development and Engineering., ECBC-TR-485
99. Kuperman RG, Checkai RT, Simini M, Phillips CT, Anthony JS, Kolakowski JE, Davis EA (2006) Toxicity of emerging energetic soil contaminant CL-20 to potworm *Enchytraeus crypticus* in freshly amended or weathered and aged treatments. *Chemosphere* 62(8):1282–1293

Additional Scholarly Articles for Further Reading

100. Agrawal JP, Walley SM, Field JE (1998) A high-speed photographic study of the impact initiation of hexanitro-hexaazaisowurtzitane and nitrotriazolone. *Combust Flame* 112(1/2):62–72. doi:[10.1016/S0010-2180\(97\)81757-9](https://doi.org/10.1016/S0010-2180(97)81757-9)
101. Aldoshin SM, Aliev ZG, Goncharov TK (2014) Crystal structure of 2,4,6,8,10,12-hexanitro-2,4,6,8,10,12-hexaazaisowurtzitane solvate with ϵ -caprolactam. *J Struct Chem* 55(4):709–712. doi:[10.1134/S0022476614040179](https://doi.org/10.1134/S0022476614040179)
102. Aldoshin SM, Aliev ZG, Goncharov TK, Korchagin DV, Milekhin YM, Shishov NI (2011) New conformer of 2,4,6,8,10,12-hexanitro-2,4,6,8,10,12-hexaazaisowurtzitane (CL-20). Crystal and molecular structures of the CL-20 solvate with glyceryl triacetate. *Russ Chem Bull* 60(7):1394–1400. doi:[10.1007/s11172-011-0209-5](https://doi.org/10.1007/s11172-011-0209-5)
103. Aldoshin SM et al (2014) Crystal structure of cocrystals 2,4,6,8,10,12-hexanitro-2,4,6,8,10,12-hexaazatetracyclo[5.5.0.05.9.03.11]dodecane with 7H-tris-1,2,5-oxadiazolo(3,4-b:3',4'-d:3",4"-f)azepine. *J Struct Chem* 55(2):327–331. doi:[10.1134/S0022476614020206](https://doi.org/10.1134/S0022476614020206)
104. Alnemrat S, Hooper JP (2013) Predicting temperature-dependent solid vapor pressures of explosives and related compounds using a quantum mechanical continuum solvation model. *J Phys Chem A* 117(9):2035–2043. doi:[10.1021/jp400164j](https://doi.org/10.1021/jp400164j)

105. Alnemrat S, Hooper JP (2014) Predicting solubility of military, homemade, and green explosives in pure and saline water using COSMO-RS. *Propellants, Explos, Pyrotech* 39 (1):79–89. doi:[10.1002/prep.201300071](https://doi.org/10.1002/prep.201300071)
106. Ammon HL (2008) Updated atom/functional group and atom_code volume additivity parameters for the calculation of crystal densities of single molecules, organic salts, and multi-fragment materials containing H, C, B, N, O, F, S, P, Cl, Br, and I. *Propellants, Explos, Pyrotech* 33(2):92–102. doi:[10.1002/prep.200700054](https://doi.org/10.1002/prep.200700054)
107. Amwele HR, Papirom P, Chukanhom K, Beamish FHW, Petkam R (2015) Acute and subchronic toxicity of metal complex azo acid dye and anionic surfactant oil on fish *Oreochromis niloticus*. *J Environ Biol* 36(1):199–205, 7p
108. Andelkovic-Lukic M (2000) New high explosive—polycyclic nitramine hexanitrohexaazaisowurtzitane (HNIW, CL-20). *Naucno-Teh Pregl* 50(6):60–64
109. Anderson SR, am Ende DJ, Salan JS, Samuels P (2014) Preparation of an energetic-energetic cocrystal using resonant acoustic mixing. *Propellants, Explos, Pyrotech* 39(5):637–640 doi:[10.1002/prep.201400092](https://doi.org/10.1002/prep.201400092)
110. Atwood AI et al (1999) Burning rate of solid propellant ingredients, part 1: pressure and initial temperature effects. *J Propul Power* 15(6):740–747. doi:[10.2514/2.5522](https://doi.org/10.2514/2.5522)
111. Paromov AE, Sysolyatin SV, Gatilov YV (2016) An acid-catalyzed cascade synthesis of oxaazatetracyclo [5.5.0.0^{3,11}.0^{5,9}]dodecane derivatives. *J Energ Mater*. doi:[10.1080/07370652.2016.1194499](https://doi.org/10.1080/07370652.2016.1194499)
112. Atwood AI et al (1999) Burning rate of solid propellant ingredients, part 2: determination of burning rate temperature sensitivity. *J Propul Power* 15(6):748–752. doi:[10.2514/2.5523](https://doi.org/10.2514/2.5523)
113. Aubuchon CM, Rector KD, Holmes W, Fayer MD (1999) Nitro group asymmetric stretching mode lifetimes of molecules used in energetic materials. *Chem Phys Lett* 299(1):84–90. doi:[10.1016/S0009-2614\(98\)01241-X](https://doi.org/10.1016/S0009-2614(98)01241-X)
114. Balakrishnan VK, Halasz A, Hawari J (2003) Alkaline Hydrolysis of the cyclic nitramine explosives RDX, HMX, and CL-20: new insights into degradation pathways obtained by the observation of novel intermediates. *Environ Sci Technol* 37(9):1838–1843. doi:[10.1021/es020959h](https://doi.org/10.1021/es020959h)
115. Balakrishnan VK, Monteil-Rivera F, Gautier MA, Hawari J (2004) Sorption and stability of the polycyclic nitramine explosive CL-20 in soil. *J Environ Qual* 33(4):1362–1368. doi:[10.2134/jeq2004.1362](https://doi.org/10.2134/jeq2004.1362)
116. Balakrishnan VK, Monteil-Rivera F, Halasz A, Corbeanu A, Hawari J (2004) Decomposition of the polycyclic nitramine explosive, CL-20, by FeO. *Environ Sci Technol* 38(24):6861–6866. doi:[10.1021/es049423h](https://doi.org/10.1021/es049423h)
117. Bardai G, Sunahara GI, Spear PA, Martel M, Gong P, Hawari J (2005) Effects of dietary administration of CL-20 on Japanese Quail *Coturnix coturnix japonica*. *Arch Environ Contam Toxicol* 49(2):215–222. doi:[10.1007/s00244-004-0231-9](https://doi.org/10.1007/s00244-004-0231-9)
118. Bardai GK et al (2006) In vitro degradation of hexanitrohexaazaisowurtzitane (CL-20) by cytosolic enzymes of Japanese quail and the rabbit. *Environ Toxicol Chem* 25(12):3221–3229. doi:[10.1897/06-068R.1](https://doi.org/10.1897/06-068R.1)
119. Bayat Y et al (2013) Synthesis of 2,4,6,8,10,12-Hexanitro-2,4,6,8,10,12-hexaazaisowurtzitane using Melaminium-tris(hydrogensulfate) by a Simple One-pot Nitration Procedure. *Propellants, Explos, Pyrotech* 38(6):745–747. doi:[10.1002/prep.201300034](https://doi.org/10.1002/prep.201300034)
120. Bayat Y, Mokhtari J, Farhadian N, Bayat M (2012) Heteropolyacids: an efficient catalyst for synthesis of CL-20. *J Energ Mater* 30(2):124–134. doi:[10.1080/07370652.2010.549539](https://doi.org/10.1080/07370652.2010.549539)
121. Bayat Y, Pourmortazavi SM, Ahadi H, Iravani H (2013) Taguchi robust design to optimize supercritical carbon dioxide anti-solvent process for preparation of 2,4,6,8,10,12-hexanitro-2,4,6,8,10,12-hexaazaisowurtzitane nanoparticles. *Chem Eng J* 230:432–438 doi:[10.1016/j.cej.2013.06.100](https://doi.org/10.1016/j.cej.2013.06.100)
122. Bayat Y, Soleyman R, Zarandi M (2015) Synthesis and characterization of novel 2,4,6,8,10,12-hexanitro-2,4,6,8,10,12-hexaazaisowurtzitane (2,4,6,8,10,12-hexanitro-2,4,6,8,10,12-hexaazatetracyclo dodecane based nanopolymer-bonded explosives by microemulsion. *J Mol Liq* 206:190–194. doi:[10.1016/j.molliq.2015.02.019](https://doi.org/10.1016/j.molliq.2015.02.019)

123. Bazaki H, Kawabe S, Miya H, Kodama T (1998) Synthesis and sensitivity of hexanitrohexaazaisowurtzitane (HNIW). *Propellants, Explos, Pyrotech* 23(6):333–336. doi:[10.1002/\(SICI\)1521-4087\(199812\)23:6<333::AID-PREP333>3.0.CO;2-X](https://doi.org/10.1002/(SICI)1521-4087(199812)23:6<333::AID-PREP333>3.0.CO;2-X)
124. Behler KD, Pesce-Rodriguez R, Cabalo J, Sausa R (2013) Infrared spectroscopy and density functional theory of crystalline β -2,4,6,8,10,12-hexanitrohexaazaisowurtzitane (β CL-20) in the region of its C-H stretching vibrations. *Spectrochim Acta, Part A* 114:708–712. doi:[10.1016/j.saa.2013.05.075](https://doi.org/10.1016/j.saa.2013.05.075)
125. Behrens R (2005) Thermal decomposition processes of energetic materials in the condensed phase at low and moderate temperatures. *Adv Ser Phys Chem* 16(Overviews of Recent Research on Energetic Materials):29–73
126. Bhushan B, Halasz A, Hawari J (2004) Nitroreductase catalyzed biotransformation of CL-20. *Biochem Biophys Res Commun* 322(1):271–276. doi:[10.1016/j.bbrc.2004.07.115](https://doi.org/10.1016/j.bbrc.2004.07.115)
127. Bhushan B, Halasz A, Spain JC, Hawari J (2004) Initial reaction(s) in biotransformation of CL-20 is catalyzed by salicylate 1-monooxygenase from *Pseudomonas* sp. strain ATCC 29352. *Appl Environ Microbiol* 70(7):4040–4047. doi:[10.1128/AEM.70.7.4040-4047.2004](https://doi.org/10.1128/AEM.70.7.4040-4047.2004)
128. Bhushan B, Halasz A, Thiboutot S, Ampleman G, Hawari J (2004) Chemotaxis-mediated biodegradation of cyclic nitramine explosives RDX, HMX, and CL-20 by *Clostridium* sp. EDB2. *Biochem Biophys Res Commun* 316(3):816–821. doi:[10.1016/j.bbrc.2004.02.120](https://doi.org/10.1016/j.bbrc.2004.02.120)
129. Bolton O, Simke LR, Pagoria PF, Matzger AJ (2012) High power explosive with good sensitivity: A 2:1 cocrystal of CL-20:HMX. *Cryst Growth Des* 12(9):4311–4314. doi:[10.1021/cg3010882](https://doi.org/10.1021/cg3010882)
130. Bonin PML, Bejan D, Radovic-Hrapovic Z, Halasz A, Hawari J, Bunce NJ (2005) Indirect oxidation of RDX, HMX, and CL-20 cyclic nitramines in aqueous solution at boron-doped diamond electrodes. *Environ Chem* 2(2):125–129. doi:[10.1071/EN05006](https://doi.org/10.1071/EN05006)
131. Boudreau AE, Hoatson DM (2004) Halogen variations in the paleoproterozoic layered mafic-ultramafic intrusions of East Kimberley, Western Australia: implications for platinum group element mineralization. *Econ Geol* 99(5):1015–1026
132. Bresler PI (1966) Gas analyzer for determination of chlorine concentrations in gas mixtures. *Zavod Lab* 32(6):7–766
133. Bunte G, Pontius H, Kaiser M (1999) Analytical characterization of impurities or byproducts in new energetic materials. *Propellants, Explos, Pyrotech* 24(3):149–155. doi:[10.1002/\(SICI\)1521-4087\(199906\)24:03<149::AID-PREP149>3.0.CO;2-4](https://doi.org/10.1002/(SICI)1521-4087(199906)24:03<149::AID-PREP149>3.0.CO;2-4)
134. Byrd EFC, Chabalowski CF, Rice BM (2007) An Ab initio study of nitromethane, HMX, RDX, CL-20, PETN, and TATB. *Science Press*, pp 696–700
135. Byrd EFC, Rice BM (2006) Improved prediction of heats of formation of energetic materials using quantum mechanical calculations. *J Phys Chem A* 110(3):1005–1013
136. Byrd EFC, Rice BM (2007) Ab initio study of compressed 1,3,5,7-tetranitro-1,3,5,7-tetraazacyclooctane (HMX), cyclotrimethylenetrinitramine (RDX), 2,4,6,8,10,12-hexanitrohexaazaisowurtzitane (CL-20), 2,4,6-trinitro-1,3,5-benzenetriamine (TATB), and pentaerythritol tetranitrate (PETN). *J Phys Chem C* 111(6):2787–2796. doi:[10.1021/jp0617930](https://doi.org/10.1021/jp0617930)
137. Bywater WG, Coleman WR, Kamm O, Merritt HH (1945) Synthetic anticonvulsants. Preparation and properties of some benzoxazoles. *J Am Chem Soc* 67:7–905. doi:[10.1021/ja01222a008](https://doi.org/10.1021/ja01222a008)
138. Campbell JA, Szecsody JE, Devary BJ, Valenzuela BR (2007) Electrospray ionization mass spectrometry of hexanitrohexaazaisowurtzitane (CL-20). *Anal Lett* 40(10):1972–1978. doi:[10.1080/00032710701484459](https://doi.org/10.1080/00032710701484459)
139. Chambers RD, Musgrave WKR, Urban PG (1975) Chlorination of perfluorodiazines. *J Fluorine Chem* 5(3):6–275. doi:[10.1016/S0022-1139\(00\)82489-6](https://doi.org/10.1016/S0022-1139(00)82489-6)
140. Chan RKS, Anselmo KJ, Reynolds CE, Worman CH (1978) Diffusion of vinyl chloride from PVC packaging material into food simulating solvents. *Polym Eng Sci* 18(7):6–601. doi:[10.1002/pen.760180709](https://doi.org/10.1002/pen.760180709)
141. Chang C-L, Lee J-S, Hsu C-K, Shieh B (2001) Thermal decomposition properties of CL-20 and NTO. *Proc NATAS Annu Conf Therm Anal Appl* 29th:685–690

142. Chapman RD, Hollins RA (2008) Benzylamine-Free, heavy-metal-free synthesis of CL-20 via hexa(1-propenyl)hexaazaisowurtzitane. *J Energ Mater* 26(4):246–273. doi:[10.1080/07370650802182385](https://doi.org/10.1080/07370650802182385)
143. Chernyshev EA, Mironov VF, Petrov AD (1960) New method of preparation of organosilicon monomers by high temperature condensation of alkenyl chlorides, aryl chlorides, and olefins with hydrosilanes. *Izv Akad Nauk SSSR, Ser Khim*:2147–2156
144. Chung K-H, Kil H-S, Choi I-Y, Chu C-K, Lee I-M (2000) New precursors for hexanitrohexaazaisowurtzitane (HNIW, CL-20). *J Heterocycl Chem* 37(6):1647–1649. doi:[10.1002/jhet.5570370640](https://doi.org/10.1002/jhet.5570370640)
145. Clawson JS, Anderson KL, Pugmire RJ, Grant DM (2004) 15 N NMR Chemical Shift Tensors of Substituted Hexaazaisowurtzitanes: The Intermediates in the Synthesis of CL-20. *J Phys Chem A* 108(14):2638–2644. doi:[10.1021/jp0373999](https://doi.org/10.1021/jp0373999)
146. Collet C, Dervaux M, Werschine M (2011) B2514A: a novel enhanced blast explosive. *Proc Int Pyrotech Semin 37th(EUROPYRO 2011)*:72–84
147. Crocker FH, Indest KJ, Fredrickson HL (2006) Biodegradation of the cyclic nitramine explosives RDX, HMX, and CL-20. *Appl Microbiol Biotechnol* 73(2):274–290. doi:[10.1007/s00253-006-0588-y](https://doi.org/10.1007/s00253-006-0588-y)
148. Crocker FH, Thompson KT, Szecsody JE, Fredrickson HL (2005) Biotic and abiotic degradation of CL-20 and RDX in soils. *J Environ Qual* 34(6):2208–2216. doi:[10.2134/jeq2005.0032](https://doi.org/10.2134/jeq2005.0032)
149. DeTata D, Collins P, McKinley A (2013) A fast liquid chromatography quadrupole time-of-flight mass spectrometry (LC-QToF-MS) method for the identification of organic explosives and propellants. *Forensic Sci Int* 233(1–3):63–74. doi:[10.1016/j.forsciint.2013.08.007](https://doi.org/10.1016/j.forsciint.2013.08.007)
150. Divekar CN, Sanghavi RR, Nair UR, Chakraborty TK, Sikder AK, Singh A (2010) Closed-vessel and thermal studies on triple-base gun propellants containing CL-20. *J Propul Power* 26(1):120–124. doi:[10.2514/1.40895](https://doi.org/10.2514/1.40895)
151. Doriath G (1995) Energetic insensitive propellants for solid and ducted rockets. *J Propul Power* 11(4):82–870. doi:[10.2514/3.23912](https://doi.org/10.2514/3.23912)
152. Dorofeeva OV, Suntsova MA (2015) Enthalpy of formation of CL-20. *Comput Theor Chem* 1057:54–59. doi:[10.1016/j.comptc.2015.01.015](https://doi.org/10.1016/j.comptc.2015.01.015)
153. Dubovik AV, Kozak GD, Aleshkina EA (2007) Theoretical estimation of explosion hazard of NTO, FOX-7, TNAZ, and CL-20. University of Pardubice, pp 484–495
154. Dumas S, Gauvrit JY, Lanteri P (2012) Determining the polymorphic purity of ϵ -CL20 contaminated by other polymorphs through the use of FTIR spectroscopy with PLS regression. *Propellants, Explos, Pyrotech* 37(2):230–234. doi:[10.1002/prep.200900090](https://doi.org/10.1002/prep.200900090)
155. Dziura R, Kazimierzuk R, Skupinski W, Pienkowski L, Grzelczyk S (2003) Reductive debenzilation in synthesis of hexanitrohexaazaisowurtzitane (HNIW, CL-20). *Organika*:31–43
156. Elbeih A, Zeman S, Jungova M, Vavra P (2013) Attractive nitramines and related PBXs. *Propellants, Explos, Pyrotech* 38(3):379–385. doi:[10.1002/prep.201200011](https://doi.org/10.1002/prep.201200011)
157. Fournier D, Monteil-Rivera F, Halasz A, Bhatt M, Hawari J (2006) Degradation of CL-20 by white-rot fungi. *Chemosphere* 63(1):175–181. doi:[10.1016/j.chemosphere.2005.06.052](https://doi.org/10.1016/j.chemosphere.2005.06.052)
158. Gar KA (1958) Field trials of 65% chlorten. *Org Insektofungitsidy i Gerbitsidy*:208–230
159. Geetha M, Nair UR, Sarwade DB, Gore GM, Asthana SN, Singh H (2003) Studies on CL-20: The most powerful high energy material. *J Therm Anal Calorim* 73(3):913–922
160. Ghosh M et al (2014) Probing crystal growth of ϵ - and α -CL-20 polymorphs via metastable phase transition using microscopy and vibrational spectroscopy. *Cryst Growth Des* 14(10):5053–5063. doi:[10.1021/cg500644w](https://doi.org/10.1021/cg500644w)
161. Ghule VD, Jadhav PM, Patil RS, Radhakrishnan S, Soman T (2010) Quantum-chemical studies on hexaazaisowurtzitanes. *J Phys Chem A* 114(1):498–503. doi:[10.1021/jp9071839](https://doi.org/10.1021/jp9071839)
162. Gnirke AU, Weidle UH (1998) Investigation of prevalence and regulation of expression of progression associated protein (PAP). *Anticancer Res* 18(6A):4363–4369
163. Gnirke AU, Weidle UH (1998) Investigation of prevalence and regulation of expression of progression associated protein (PAP). *Anticancer Res* 18(6A):4363–4369

164. Goede P, Latypov NV, Oestmark H (2004) Fourier transform Raman Spectroscopy of the four crystallographic phases of α , β , γ and ϵ 2,4,6,8,10,12-hexanitro-2,4,6,8,10,12-hexaazatetracyclo[5.5.0.0.05.9.03.11]dodecane (HNIW, CL-20). *Propellants, Explos, Pyrotech* 29(4):205–208 doi:[10.1002/prop.200400047](https://doi.org/10.1002/prop.200400047)
165. Golofit T, Zysk K (2015) Thermal decomposition properties and compatibility of CL-20 with binders HTPB, PBAN, GAP and polyNIMMO. *J Therm Anal Calorim* 119(3):1931–1939. doi:[10.1007/s10973-015-4418-2](https://doi.org/10.1007/s10973-015-4418-2)
166. Gong P, Sunahara GI, Rocheleau S, Dodard SG, Robidoux PY, Hawari J (2004) Preliminary ecotoxicological characterization of a new energetic substance, CL-20. *Chemosphere* 56 (7):653–658. doi:[10.1016/j.chemosphere.2004.04.010](https://doi.org/10.1016/j.chemosphere.2004.04.010)
167. Granito C, Schultz HP (1963) Decarboxylation studies. II. Preparation of alkyl phenyl ketones. *J Org Chem* 28:81–879. doi:[10.1021/jo01038a521](https://doi.org/10.1021/jo01038a521)
168. Greenberg BL, Kalyon DM, Erol M, Mezger M, Lee K, Lusk S (2003) Analysis of slurry-coating effectiveness of CL-20 using grazing incidence x-ray diffraction. *J Energ Mater* 21(3):185–199. doi:[10.1080/716100383](https://doi.org/10.1080/716100383)
169. Groom CA, Halasz A, Paquet L, D'Cruz P, Hawari J (2003) Cyclodextrin-assisted capillary electrophoresis for determination of the cyclic nitramine explosives RDX, HMX and CL-20. Comparison with high-performance liquid chromatography. *J Chromatogr, A* 999(1–2):17–22 doi:[10.1016/S0021-9673\(03\)00389-3](https://doi.org/10.1016/S0021-9673(03)00389-3)
170. Hakansson K, Coorey RV, Zubarev RA, Talrose VL, Hakansson P (2000) Low-mass ions observed in plasma desorption mass spectrometry of high explosives. *J Mass Spectrom* 35 (3):337–346
171. Hawari J, Deschamps S, Beaulieu C, Paquet L, Halasz A (2004) Photodegradation of CL-20: insights into the mechanisms of initial reactions and environmental fate. *Water Res* 38 (19):4055–4064. doi:[10.1016/j.watres.2004.06.032](https://doi.org/10.1016/j.watres.2004.06.032)
172. Hoffmann RW, Sieber W, Guhn G (1965) Decomposition of 1,2,3-benzothiadiazole 1,1-dioxide. *Chem Ber* 98(11):8–3470
173. Hultquist ME et al (1951) N-Heterocyclic benzenesulfonamides. *J Am Chem Soc* 73:66–2558. doi:[10.1021/ja01150a042](https://doi.org/10.1021/ja01150a042)
174. Isayev O, Gorb L, Qasim M, Leszczynski J (2008) Ab initio molecular dynamics study on the initial chemical events in nitramines: thermal decomposition of CL-20. *J Phys Chem B* 112(35):11005–11013. doi:[10.1021/jp804765m](https://doi.org/10.1021/jp804765m)
175. Kaste PJ, Rice BM (2004) Novel energetic materials for the future force: the army pursues the next generation of propellants and explosives. *AMPTIAC Q* 8(4):85–89
176. Keshavarz MH, Yousefi MH (2008) Heats of sublimation of nitramines based on simple parameters. *J Hazard Mater* 152(3):929–933. doi:[10.1016/j.jhazmat.2007.07.067](https://doi.org/10.1016/j.jhazmat.2007.07.067)
177. Kholod Y et al (2006) Are 1,5- and 1,7-dihydrodiimidazo[4,5-b:4',5'-e]pyrazine the main products of 2,4,6,8,10,12-hexanitro-2,4,6,8,10,12-hexaazaisowurtzitane (CL-20) alkaline hydrolysis? A DFT study of vibrational spectra. *J Mol Struct* 794(1–3):288–302. doi:[10.1016/j.molstruc.2006.02.061](https://doi.org/10.1016/j.molstruc.2006.02.061)
178. Kholod Y, Kosenkov D, Okovytyy S, Gorb L, Qasim M, Leszczynski J (2008) CL-20 photodecomposition: Ab initio foundations for identification of products. *Spectrochim Acta, Part A* 71A(1):230–237. doi:[10.1016/j.saa.2007.12.021](https://doi.org/10.1016/j.saa.2007.12.021)
179. Kim J-H, Park Y-C, Yim Y-J, Han J-S (1998) Crystallization behavior of hexanitrohexaazaisowurtzitane at 298 K and quantitative analysis of mixtures of its polymorphs by FTIR. *J Chem Eng Jpn* 31(3):478–481. doi:[10.1252/jcej.31.478](https://doi.org/10.1252/jcej.31.478)
180. Kim J-H, Park Y-C, Yim Y-J, Han J-S (1998) Crystallization behavior of hexanitrohexaazaisowurtzitane at 298 K and quantitative analysis of mixtures of its polymorphs by FTIR. *J Chem Eng Jpn* 31(3):478–481. doi:[10.1252/jcej.31.478](https://doi.org/10.1252/jcej.31.478)
181. Klapotke TM, Ang H-G (2001) Estimation of the crystalline density of nitramine (N-NO₂ based) high energy density materials (HEDM). *Propellants, Explos, Pyrotech* 26(5):221–224. doi:[10.1002/1521-4087\(200112\)26:5<221::AID-PREP221>3.0.CO;2-T](https://doi.org/10.1002/1521-4087(200112)26:5<221::AID-PREP221>3.0.CO;2-T)
182. Klapötke TM, Witkowski TG (2016) Covalent and Ionic Insensitive High-Explosives. *Propellants, Explos, Pyrotech* 41:470–483. doi:[10.1002/prop.201600006](https://doi.org/10.1002/prop.201600006)

183. Knox-Holmes B (1993) Biofouling control with low levels of copper and chlorine. *Biofouling* 7(2):66–157. doi:[10.1080/08927019309386250](https://doi.org/10.1080/08927019309386250)
184. Koslik P, Stas J, Wilk Z, Zakrzewski A (2007) Research of high explosives based on RDX, HMX and CL-20 in the small scale underwater test examination. *Cent Eur J Energ Mater* 4 (3):3–13
185. Koutsospyros A, Christodoulatos C, Panikov N, Malcheva O, Karakaya P, Nicolich S (2004) Environmental relevance of CL-20: preliminary findings. *Water Air Soil Pollut Focus* 4(4–5):459–470. doi:[10.1023/B:WAFO.0000044818.76609.e9](https://doi.org/10.1023/B:WAFO.0000044818.76609.e9)
186. Li H, Shu Y, Gao S, Chen L, Ma Q, Ju X (2013) Easy methods to study the smart energetic TNT/CL-20 co-crystal. *J Mol Model* 19(11):4909–4917. doi:[10.1007/s00894-013-1988-4](https://doi.org/10.1007/s00894-013-1988-4)
187. Li J, Brill TB (2007) Kinetics of solid polymorphic phase transitions of CL-20. *Propellants, Explos, Pyrotech* 32(4):326–330. doi:[10.1002/prop.200700036](https://doi.org/10.1002/prop.200700036)
188. Lizlovs EA, Bond AP (1975) Effect of low-temperature aging on corrosion resistance of chromium-molybdenum (18Cr-2Mo) titanium-stabilized ferritic stainless steel. *J Electrochem Soc* 122(5):93–589. doi:[10.1149/1.12134271](https://doi.org/10.1149/1.12134271)
189. Maksimowski P, Skupinski W, Szczypińska J (2013) Comparison of the crystals obtained by precipitation of CL-20 with different chemical purity. *Propellants, Explos, Pyrotech* 38 (6):791–797. doi:[10.1002/prop.201300064](https://doi.org/10.1002/prop.201300064)
190. Marvin KW, Fujimoto W, Jetten AM (1995) Identification and characterization of a novel squamous cell-associated gene related to PMP22. *J Biol Chem* 270(48):16–28910. doi:[10.1074/jbc.270.48.28910](https://doi.org/10.1074/jbc.270.48.28910)
191. Mathieu J, Stucki H (2004) Military high explosives. *Chimia* 58(6):383–389. doi:[10.2533/000094290477767669](https://doi.org/10.2533/000094290477767669)
192. Meents A, Dittrich B, Johnas SKJ, Thome V, Weckert EF (2008) Charge-density studies of energetic materials: CL-20 and FOX-7. *Acta Crystallogr Sect B: Struct Sci* 64(4):519. doi:[10.1107/S0108768108017497](https://doi.org/10.1107/S0108768108017497)
193. Millar DIA et al (2012) Crystal engineering of energetic materials: Co-crystals of CL-20. *CrystEngComm* 14(10):3742–3749. doi:[10.1039/c2ce05796d](https://doi.org/10.1039/c2ce05796d)
194. Molt RW, Bartlett RJ, Watson T, Bazante AP (2012) Conformers of CL-20 explosive and ab initio refinement using perturbation theory: implications to detonation mechanisms. *J Phys Chem A* 116(49):12129–12135. doi:[10.1021/jp305443h](https://doi.org/10.1021/jp305443h)
195. Monteil-Rivera F et al (2009) Fate of CL-20 in sandy soils: degradation products as potential markers of natural attenuation. *Environ Pollut* 157(1):77–85
196. Naik NH, Gore GM, Gandhe BR, Sikder AK (2008) Studies on thermal decomposition mechanism of CL-20 by pyrolysis gas chromatography-mass spectrometry (Py-GC/MS). *J Hazard Mater* 159(2–3):630–635. doi:[10.1016/j.jhazmat.2008.02.049](https://doi.org/10.1016/j.jhazmat.2008.02.049)
197. Namasivayam C, Kanagarathinam A (1992) Distillery wastewater treatment using waste iron (3+)/chromium(3+) hydroxide sludge and polymer flocculants. *J Environ Sci Health, Part A* 27(7):37–1721
198. Nedelko VV et al (2000) Comparative investigation of thermal decomposition of various modifications of hexanitrohexaazaisowurtzitane (CL-20). *Propellants, Explos, Pyrotech* 25 (5):255–259. doi:[10.1002/1521-4087\(200011\)25:5<255:AID-PREP255>3.0.CO;2-8](https://doi.org/10.1002/1521-4087(200011)25:5<255:AID-PREP255>3.0.CO;2-8)
199. Oehrle SA (1996) Analysis of nitramine and nitroaromatic explosives by micellar electrokinetic capillary chromatography (MECC). *J Energ Mater* 14(1):47–56. doi:[10.1080/07370659608216057](https://doi.org/10.1080/07370659608216057)
200. Ogata Y, Kawasaki A, Nakagawa K (1964) Kinetics of the formation of benzoguanamine from dicyandiamide and benzonitrile. *Tetrahedron* 20(12):61–2755. doi:[10.1016/S0040-4020\(01\)98493-5](https://doi.org/10.1016/S0040-4020(01)98493-5)
201. Okovytyy S, Kholod Y, Qasim M, Fredrickson H, Leszczynski J (2005) The Mechanism of Unimolecular Decomposition of 2,4,6,8,10,12-Hexanitro-2,4,6,8,10,12-hexaazaisowurtzitane. A computational DFT study. *J Phys Chem A* 109(12):2964–2970. doi:[10.1021/jp045292v](https://doi.org/10.1021/jp045292v)
202. Patel AR, Oneto JF (1963) Basic 1,3-dioxolanes. *J Pharm Sci* 52(6):92–588. doi:[10.1002/jps.2600520618](https://doi.org/10.1002/jps.2600520618)

203. Paulin A, Jobson BA, Vukcevic S (1981) Chlorination of alumina-containing materials in fluidized bed. *Trav Com Int Etude Bauxites, Alumine Alum* 16:70–161
204. Peralta-Inga Z, Degirmenbasi N, Olgun U, Gocmez H, Kalyon DM (2006) Recrystallization of CL-20 and HNFx from solution for rigorous control of the polymorph type: part I, mathematical modeling using molecular dynamics method. *J Energ Mater* 24(2):69–101. doi:[10.1080/07370650600672082](https://doi.org/10.1080/07370650600672082)
205. Pivina T, Korolev V, Khakimov D, Petukhova T, Ivshin V, Lempert D (2012) Computer simulation of decomposition mechanisms for CL-20, hydrazine, and their binary system. *Propellants, Explos, Pyrotech* 37(4):502–509. doi:[10.1002/prop.201100098](https://doi.org/10.1002/prop.201100098)
206. Reeves CC Jr, Miller WD (1978) Nitrate, chloride and dissolved solids, Ogallala aquifer, west Texas. *Ground Water* 16(3):73–167. doi:[10.1111/j.1745-6584.1978.tb03218.x](https://doi.org/10.1111/j.1745-6584.1978.tb03218.x)
207. Robidoux PY et al (2004) Acute and chronic toxicity of the new explosive CL-20 to the earthworm (*Eisenia andrei*) exposed to amended natural soils. *Environ Toxicol Chem* 23 (4):1026–1034. doi:[10.1897/03-308](https://doi.org/10.1897/03-308)
208. Sandor A (1964) Thermionic emission from barium-coated ultrapure nickel in the emission microscope. *J Electron Control* 17(4):91–377. doi:[10.1080/00207216408937712](https://doi.org/10.1080/00207216408937712)
209. Sandor A (1964) Thermionic emission from barium-coated ultrapure nickel in the emission microscope. *J Electron Control* 17(4):91–377. doi:[10.1080/00207216408937712](https://doi.org/10.1080/00207216408937712)
210. Sausa RC, Cabalo JB (2012) The detection of energetic materials by laser photoacoustic overtone spectroscopy. *Appl Spectrosc* 66(9):993–998. doi:[10.1366/12-06699](https://doi.org/10.1366/12-06699)
211. Schefflan R, Kovenklioglu S, Kalyon D, Redner P, Heider E (2006) Mathematical model for a fed-batch crystallization process for energetic crystals to achieve targeted size distributions. *J Energ Mater* 24(2):157–172. doi:[10.1080/07370650600672058](https://doi.org/10.1080/07370650600672058)
212. Sikder AK, Sikder N, Gandhe BR, Agrawal JP, Singh H (2002) Hexanitrohexaazaisowurtzitane or CL-20 in India: synthesis and characterisation. *Def Sci J* 52(2):135–146
213. Sinditskii VP, Burzhava AV, Sheremetev AB, Aleksandrova NS (2012) Thermal and combustion properties of 3,4-bis(3-nitrofurazan-4-yl)furoxan (DNF). *Propellants, Explos, Pyrotech* 37(5):575–580. doi:[10.1002/prop.201100095](https://doi.org/10.1002/prop.201100095)
214. Sinditskii VP, Egorshv VV, Serushkin VV, Filatov SA, Chernyi AN (2012) Combustion mechanism of energetic binders with nitramines. *Int J Energ Mater Chem Propul* 11(5):427–449. doi:[10.1615/IntJEnergeticMaterialsChemProp.2013005557](https://doi.org/10.1615/IntJEnergeticMaterialsChemProp.2013005557)
215. Singh H (2005) Current trend of R&D in the field of high energy materials: an overview. *Explosion* 15(3):120–132
216. Sivabalan R, Gore GM, Nair UR, Saikia A, Venugopalan S, Gandhe BR (2007) Study on ultrasound assisted precipitation of CL-20 and its effect on morphology and sensitivity. *J Hazard Mater* 139(2):199–203. doi:[10.1016/j.jhazmat.2006.06.027](https://doi.org/10.1016/j.jhazmat.2006.06.027)
217. Souers PC et al (2001) Detonation energies from the cylinder test and CHEETAH V3.0. *Propellants, Explos, Pyrotech* 26(4):180–190 doi:[10.1002/1521-4087\(200110\)26:4<180::AID-PREP180>3.0.CO;2-K](https://doi.org/10.1002/1521-4087(200110)26:4<180::AID-PREP180>3.0.CO;2-K)
218. Steinmetz I, Rott L, Boer C (1966) Enrichment of ground waters with surface waters. *Hydrobiologia* 7:195–201
219. Strigul N, Braid W, Christodoulatos C, Balas W, Nicolich S (2005) The assessment of the energetic compound 2,4,6,8,10,12-hexanitro-2,4,6,8,10,12-hexaazaisowurtzitane (CL-20) degradability in soil. *Environ Pollut* 139(2):353–361. doi:[10.1016/j.envpol.2005.05.002](https://doi.org/10.1016/j.envpol.2005.05.002)
220. Suzuki J et al (1984) Performance of Shimadzu clinical chemistry analyzer CL-20. *Shimadzu Hyoron* 41(4):45–229
221. Szecsody JE, Girvin DC, Devary BJ, Campbell JA (2004) Sorption and oxic degradation of the explosive CL-20 during transport in subsurface sediments. *Chemosphere* 56(6):593–610. doi:[10.1016/j.chemosphere.2004.04.028](https://doi.org/10.1016/j.chemosphere.2004.04.028)
222. Talawar MB et al (2006) Effect of organic additives on the mitigation of volatility of 1-nitro-3,3'-dinitroazetidine (TNAZ): Next generation powerful melt castable high energy material. *J Hazard Mater* 134(1–3):8–18. doi:[10.1016/j.jhazmat.2003.10.008](https://doi.org/10.1016/j.jhazmat.2003.10.008)
223. Talawar MB, Sivabalan R, Polke BG, Nair UR, Gore GM, Asthana SN (2005) Establishment of process technology for the manufacture of dinitrogen pentoxide and its utility for the

- synthesis of most powerful explosive of today—CL-20. *J Hazard Mater* 124(1–3):153–164. doi:[10.1016/j.jhazmat.2005.04.021](https://doi.org/10.1016/j.jhazmat.2005.04.021)
224. Tappan AS, Basiliere M, Ball JP, Snedigar S, Fischer GJ, Salton J (2010) Linear actuation using milligram quantities of CL-20 and TAGDNAT. *Propellants, Explos, Pyrotech* 35 (3):207–212. doi:[10.1002/prop.201000025](https://doi.org/10.1002/prop.201000025)
 225. Tappan BC, Brill TB (2003) Thermal decomposition of energetic materials 86. Cryogel synthesis of nanocrystalline CL-20 coated with cured nitrocellulose. *Propellants, Explos, Pyrotech* 28(5):223–230 doi:[10.1002/prop.200300009](https://doi.org/10.1002/prop.200300009)
 226. Thiboutot S, Brousseau P, Ampleman G, Pantea D, Cote S (2008) Potential use of CL-20 in TNT/ETPE-based melt cast formulations. *Propellants, Explos, Pyrotech* 33(2):103–108. doi:[10.1002/prop.200700223](https://doi.org/10.1002/prop.200700223)
 227. Tian Q et al (2013) Thermally induced damage in hexanitrohexaazaisowurtzitane. *Cent Eur J Energ Mater* 10(3):359–369
 228. Tomas-Alonso F, Rubio AM, Alvarez R, Ortuno JA (2013) Dynamic potential response and SEM-EDX studies of polymeric inclusion membranes based on ionic liquids. *Int J Electrochem Sci* 8(4):4955–4969
 229. Urbelis JH, Young VG, Swift JA (2015) Using solvent effects to guide the design of a CL-20 cocrystal. *CrystEngComm* 17(7):1564–1568. doi:[10.1039/C4CE02285H](https://doi.org/10.1039/C4CE02285H)
 230. Van der Heijden AEDM (1998) Crystallization and characterization of energetic materials. *Curr Top Cryst Growth Res* 4:99–114
 231. van der Heijden AEDM, Bouma RHB, van der Steen AC (2004) Physicochemical parameters of nitramines influencing shock sensitivity. *Propellants, Explos, Pyrotech* 29 (5):304–313. doi:[10.1002/prop.200400058](https://doi.org/10.1002/prop.200400058)
 232. van der Heijden AEDM, Bouma RHB, van der Steen AC (2004) Physicochemical parameters of nitramines influencing shock sensitivity. *Propellants, Explos, Pyrotech* 29 (5):304–313. doi:[10.1002/prop.200400058](https://doi.org/10.1002/prop.200400058)
 233. Viswanath DS, Reinig M, Ghosh TK, Boddu VM (2010) Vapor pressure of nitro compounds, vol Pt. 1. University of Pardubice, Institute of Energetic Materials, pp 306–309
 234. Viswanath JV, Venugopal KJ, Rao NVS, Venkataraman A (2016) An overview on importance, synthetic strategies and studies of 2,4,6,8,10,12-hexanitro-2,4,6,8,10,12-hexaazaisowurtzitane (HNIW). *Defence Technol* 12(5), October 2016, pp 401–418
 235. Volk F, Bathelt H (1997) Influence of energetic materials on the energy-output of gun propellants. *Propellants, Explos, Pyrotech* 22(3):120–124. doi:[10.1002/prop.19970220305](https://doi.org/10.1002/prop.19970220305)
 236. Volk F, Bathelt H (1995) Influence of energetic materials on the energy-output of gun propellants. *Am Defense Preparedness Assoc*: 82–89
 237. von Holtz E, Ornellas D, Foltz MF, Clarkson JE (1994) The solubility of ϵ -CL-20 in selected materials. *Propellants, Explos, Pyrotech* 19(4):12–206. doi:[10.1002/prop.19940190410](https://doi.org/10.1002/prop.19940190410)
 238. Wu Y, Ou Y, Liu Z, Liu J, Meng Z, Chen B (2004) Theoretical studies on the possible conformers and properties of tetranitrodiazidoacetylhexaazaisowurtzitane (TNDAIW). *Sci China, Ser B: Chem* 47(5):414–419. doi:[10.1360/04yb0046](https://doi.org/10.1360/04yb0046)
 239. Xing X et al (2015) Thermal decomposition behavior of hexanitrohexaazaisowurtzitane and its blending with BTATz (expand) and Al by microcalorimetry. *J Therm Anal Calorim: Ahead of Print*. doi:[10.1007/s10973-015-4431-5](https://doi.org/10.1007/s10973-015-4431-5)
 240. Yazici R, Kalyon D (2005) Microstrain and defect analysis of CL-20 crystals by novel x-ray methods. *J Energ Mater* 23(1):43–58. doi:[10.1080/07370650590920287](https://doi.org/10.1080/07370650590920287)
 241. Zhang C et al (2014) Evident hydrogen bonded chains building CL-20-based cocrystals. *Cryst Growth Des* 14(8):3923–3928. doi:[10.1021/cg500796r](https://doi.org/10.1021/cg500796r)
 242. Zhang P, Guo X-Y, Zhang J-Y, Jiao Q-J (2014) Application of liquid paraffin in castable CL-20-based PBX. *J Energ Mater* 32(4):278–292. doi:[10.1080/07370652.2013.862318](https://doi.org/10.1080/07370652.2013.862318)
 243. Zubarev RA, Hakansson P, Hakansson K, Talrose VL (1998) Matrix assisted particle desorption techniques: use of explosive matrixes. *Adv Mass Spectrom* 14:B061920/1–B061920/8

Emerging Energetic Materials: Synthesis,
Physicochemical, and Detonation Properties

Viswanath, D.S.; Ghosh, T.K.; Boddu, V.M.

2018, XI, 478 p. 134 illus., 13 illus. in color., Hardcover

ISBN: 978-94-024-1199-7